CHARLES UNIVERSITY

FACULTY OF PHARMACY IN HRADEC KRÁLOVÉ

DEPARTMENT OF PHARMACOGNOSY AND PHARMACEUTICAL BOTANY

MASTER'S THESIS

Amaryllidaceae alkaloids of *Narcissus poeticus* var. *recurvus* and their implication to Alzheimer's disease and anticancer activity

Supervisor: PharmDr. Daniela Suchánková, Ph.D.

Consultant: PharmDr. Jana Křoustková, Ph.D.

Head of the department: prof. Ing. Lucie Cahlíková, Ph.D.

Hradec Králové, September 2024 Simona Hašanová

Statement of authorship

I declare that this work is my original piece of writing, which I completed independently under the guidance of my supervisor and consultant. The complete literature and other sources that I used in the preparation are listed in the references and properly cited in the work. This work has not been used to obtain another or the same degree.

Hradec Králové,September 2024 Simona Hašanová

Acknowledgment

I would like to extend my big thanks to my supervisor, PharmDr. Daniela Suchánková, Ph.D., for welcoming me into the research group in my second year of study, for her help, advice in laboratory and time. A huge thank you goes to my consultant, PharmDr. Jana Křoustková, Ph.D., for her immense scientific enthusiasm, her ever-present smile, that uplifted me as well, her abundant scientific advice, and her time. I deeply appreciate the strong support, patience, and kindness they have shown me throughout my years in the department. I am also grateful for the numerous opportunities they provided for me to grow in academic science.

I would also like to thank the entire team at the Department of Pharmacognosy and Pharmaceutical Botany for warmly welcoming me into their group. Special thanks to Vilma and Petra, the lab technicians, who assisted me with mincing the bulbs and preparing solvents. I am grateful to Assoc. Prof. PharmDr. Jakub Chlebek, Ph.D. for his help with flash chromatography and our engaging scientific discussions; to RNDr. Jaroslav Jenčo, Ph.D, for his assistance with alkaloid structure evaluation by GC/MS and HPLC/MS; and to PharmDr. Kateřina Hradiská Breitrová, PhD. for her support and consultation on the biological activities of alkaloids. I also extend my thanks to Prof. PharmDr. Lucie Cahlíková, PhD. for giving me the opportunity to work in the department and for a great opportunity to attend the Phytochemical conference.

Special thanks are due to Assoc. Prof. PharmDr. Jiří Kuneš, CSc. and to my consultant for their NMR analysis of compounds, to Assoc. Prof. RNDr. Radim Havelek, PhD., for his cytotoxicity screening and kind communication, and to Ida Dufková for measuring antibacterial and antifungal activity. My sincere goes to Assoc. Prof. PharmDr. Ján Zitko, Ph.D., for his time, assistance, and consultations on molecular docking.

I would like to thank the team at the Department of Pharmaceutical Chemistry, Faculty of Pharmacy, University of Ljubljana, for their kind assistance and for allowing me to work with natural alkaloid samples during the Erasmus+ programme. In particular, I am grateful to Assoc. Prof. Andrej Emanuel Cotman for his kind assistance, for teaching me to survive in a synthetic laboratory, and for his help in looking for a purification method. My thanks also go to MSc. Ana Jug for measuring topoisomerase IIα inhibitory activity, and to Assistant MSc. Jaka Dernovšek for conducting the MTS assay, as well as for their kind approach and consultations. I would also like to thank MSc. Jernej Cingl and MSc. Ivan Džajić for their kindness, enthusiasm, and scientific advice.

Finally, I would like to thank my partner MUDr. Patrik Nejl for his consultations regarding Alzheimer's disease, as well as his patience and support. I also want to acknowledge the support

of all my friends and family throughout my years of hard work in the lab, especially during the challenging task of summarizing my results in this master's thesis.

Content

List of abbreviations

AAs	Amaryllidaceae alkaloids
Aβ	β-amyloid
AC	*Absidia corymbifera*
AD	Alzheimer's disease
ACh	Acetylcholine
ACI	*Acinetobacter baumannii*
AChE	Acetylcholinesterase
AChEI	Acetylcholinesterase inhibitors
AF	*Aspergillus fumigatus*
AFla	*Aspergillus flavus*
ATP	Adenosine triphosphate
BuChE	Butyrylcholinesterase
BuChEI	Butyrylcholinesterase inhibitors
CA1	*Candida albicans*
ChAT	Choline acetyltransferase enzyme
ChIs	Cholinesterase inhibitors
CK	*Candida krusei*
CO_2	Carbon dioxide
CP	*Candida parapsilosis*
CT	*Candida tropicalis*
EC	*Escherichia coli*
ED_{50}	Middle effective dose
EF	*Enterococcus faecalis*
EI	Electric ionisation
EMA	European Medicines Agency
ESI	Electric spray ionisation
FDA	Food Drug Administration
GC	Gass chromatography
GI_{50}	Grow inhibition 50%
GP	Growth percentage
GSK-3β	Glycogen synthase kinase 3β
*h*AChE	Human acetylcholinesterase
*h*BuChE	Human butyrylcholinesterase

HPLC	High performance liquid chromatography
IC_{50}	Middle inhibition concentration
KO	*Klebsiella pneumoniae*
LE	Ligand efficiency
MOE	Molecular operating environment
MP	Mobile phase
MS	Mass spectrometry
MW	Molecular weight
NIST	National Institute of Standards and Technology Library
NMDA	*N*-methyl-D-aspartate receptors
NMR	Nuclear magnetic resonance
PA	*Pseudomonas aeruginosa*
PDB	Protein data bank
POP	Prolyloligopeptidase
Rf	Retention factor
SA	*Staphylococcus aureus* subsp. *Aureus*
SBDD	Structure based drug design
SE	*Staphylococcus epidermalis*
SiO_2	Silica gel
TF	Triplex formation
TFO1	Transposon from *Fusarium oxysporum*
TI	*Trichophyton inerdigitale*
TLC	Thin layer chromatography
Topo I	Topoisomerase I
Topo IIα	Topoisomerase IIα
var.	Variety

Table 1. *List of cell line abbreviations used in Theoretical section*

Cell line	Tumour type	Cell line	Tumour type
A2780	ovarian carcinoma	**K562**	myelogenous leukemia
A549	non-small cell lung carcinoma	**KM3**	multiple myeloma
B16F10	melanoma	**LLC**	lung cancer
BJ	esophageal carcinoma	**MCF-7**	breast adenocarcinoma
C-6	glioblastoma	**MDA-MB-231**	adenocarcinoma
C8161	hepatoma	**MOLT-4**	T-lymphoblastic leukaemia
Caco-2	colon carcinoma	**NCI-H460**	lung cancer
CEM	T-lymphoblastic leukaemia	**OE21**	esophageal carcinoma
CHO-K1	ovarian carcinoma	**PC-3**	prostatic adenocarcinoma
COL-2	colon carcinoma	**SKMEL**	human melanoma
G-361	hepatoma	**SK-MEL-28**	human melanoma
HCT-15	colon carcinoma	**SK-OV-3**	ovarian carcinoma
HeLa	cervical adenocarcinoma	**SW1573**	alveolar cell carcinoma
HepG2	hepatocellular carcinoma	**T24**	human bladder carcinoma
Hey1B	ovarian carcinoma	**T47-D**	breast carcinoma
HL-60	leukaemia	**T98G**	glioblastoma
Hs578T	breast carcinoma	**U373**	human glioblastoma
Hs683	glioblastoma	**U937**	myeloid leukaemia
HT-29	colorectal adenocarcinoma		

1 Introduction

Since ancient times, natural products have been used in folklore to treat various diseases and illnesses. Many of these natural products have subsequently become current drug candidates.[1] In fact, an analysis of the pharmaceutical market reveals that 42% of clinically used substances were either primarily isolated from natural sources or prepared as semi-synthetic derivatives of natural compounds.[2] This highlights the importance of phytochemistry in drug discovery, particularly in the search for new, promising scaffolds.

Classical natural product chemistry methodologies have enabled the discovery of a vast array of bioactive secondary metabolites from terrestrial and marine sources.[1] These secondary metabolites exert significant pharmacological and toxicological effects in humans.[3] An important group of these metabolites, particularly relevant to this master's thesis, are the alkaloids, specifically the Amaryllidaceae alkaloids (AAs) found in the Amaryllidaceae family.

The Amaryllidaceae family includes 75 genera and approximately 1,100 species, many of which have a long history of medicinal use. From a phytochemical perspective, more than 500 AAs have been isolated, and they have been reported to exhibit acetylcholinesterase (AChE) inhibitory, antibacterial, antifungal, antimalarial, anti-tumour, antiviral, and cytotoxic activities.[4] These findings underscore the potential of these compounds in drug development.

Narcissus (Amaryllidaceae) flowers have been used in folk medicine for cancer management. The powerful anticancer properties of *Narcissus poeticus* were already known to Hippokrates of Kos (ca. 460-370 BC). The topical anticancer uses of extracts *N. poeticus* and *N. pseudonarcissus* were documented in the first century AD by the Roman natural philosopher Gaius Plinius Secundus (AD 23-79), better known as Pliny the Elder.[5]

This historically significant species is the subject of this master's thesis, a part of the first extensive phytochemical study on this variety. *Narcissus poeticus* var. *recurvus* (Haw.) Herb.[6] was chosen not only because of its prospective historical profile but also based on a preliminary screening study conducted at the Department of Pharmacognosy and Pharmaceutical Botany, Faculty of Pharmacy in Hradec Králové, Charles University. In this study, a promising cholinesterase inhibition profile (IC_{50} (*h*AChE) = 6.0 ± 0.1 µM; IC_{50} (*h*BuChE) = 23.0 ± 1.0 µM) was identified, which made from *N. poeticus* var. *recurvus* an interesting target for AD research.[7]

2 Aims of the master's thesis

This master's thesis was part of a comprehensive phytochemical study of the plant *Narcissus poeticus* var. *recurvus*, conducted by members of the research group at the Department of Pharmacognosy and Pharmaceutical Botany, Faculty of Pharmacy, Charles University.

The specific aims of the master's thesis are:

1. Preparation of an alkaloid extract by extracting bulbs of *Narcissus poeticus* var. *recurvus*.
2. Fractionization of alkaloid extract by flash chromatography and prediction of alkaloid content.
3. Isolation of alkaloids.
4. Structure evaluation of isolated alkaloids.
5. *In vitro* analysis of isolated alkaloids for anticancer activity and their implications for Alzheimer's disease (AD).
6. *In silico* analysis of isolated alkaloids for human acetylcholinesterase (*h*AChE) enzyme inhibition.
7. Summarization of the results and a brief review describing the topic of the master's thesis.

3 Theoretical section

3.1 Genus *Narcissus*

The genus *Narcissus* belongs to the Narcisseae, one of the 15 tribes of the Amaryllidaceae family.[8] This family comprises about 75 genera and 1100 species distributed widely in tropical regions of the world.[4]

Unlike other genera of the family, *Narcissus* has a mainly Mediterranean distribution. The genus also occurs in southwestern France, northern Africa, and eastwards to Greece. The taxonomy of *Narcissus* is difficult because of the ease with which hybridization occurs naturally, accompanied by extensive cultivation, breeding, selection, escape, and naturalisation.[9] There are approximately 80–100 wild species.[8]

3.1.1 *Narcissus poeticus*

This master's thesis deals with one specific species of this genus, *Narcissus poeticus*. This plant is widely distributed across Europe, from Spain in the west to Ukraine in the east and is naturalized in many other places. The species has large, single flowers with six white perianth segments and a central shallowly cup-shaped corona, which forms a circular ring of raised tissue within the perianth. The corona is frequently greenish at the base inside, a yellow zone above that and with a bright scarlet crenelated rim or margin.[10]

In a list of botanical names that the Royal Horticultural Society (RHS) accepted in the genus *Narcissus*, they recognized *Narcissus poeticus* with six wild varieties.[10]

Wild varieties are:

Narcissus poeticus

var. *poeticus*[11] (Southern France, Italy)[9]

var. *hellenicus* (Pugsley) A. Fernandes[11] (Greece)[9]

var. *majalis* (Curtis) A. Fernandes[11] (France)[9]

var. *recurvus* (Haworth) A. Fernandes (Switzerland)[9]

var. *verbanensis* Herbert[11] (Italy)[9]

For the purpose of this master's thesis, *Narcissus poeticus* var. *recurvus* was selected. This name comes from its recurved petals which are considered one of the whitest in the genus *Narcissus*.[10]

Figure 1. *Narcissus poeticus* var. *recurvus.*[12]

3.2 Amaryllidaceae alkaloids in the genus *Narcissus*

Since the isolation of the first Amaryllidaceae alkaloid, lycorine, from *Narcissus pseudonarcissus* by Gerrad at the end of last century,[9] more than 500 AAs have been isolated,[4] as already mentioned in the introduction. **Table 2** describes alkaloids identified in the genus *Narcissus* by studies of Bastida and Viladomat.[8]

Table 2*. Narcissus alkaloid content*[8]

Structure type	Alkaloid name
Lycorine	**lycorine**, poetaminine, pseudolycorine, 1-*O*-acetylpseudolycorine, 2-*O*-acetylpseudolycorine, 9-*O*-methylpseudolycorine, **galanthine**, goleptine, jonquilline, caranine, pluviine, norpluviine, 9-*O*-demethylpluviine, 1-*O*-acetyl-9-*O*-demethylpluviine, narcissidine, oxoassoanine, tortuosine, 1-9-*O*-diacetyl-9-*O*-demethylpluviine, nartazine, vasconine, assoanine, roserine
Homolycorine	homolycorine, hippeastrine, lycorenine, 8-*O*-demethylhomolycorine, 8-*O*-demethyl-8-*O*-acetylhomolycorine, 9-*O*-demethylhomolycorine, masonine, normasonine, 9-*O*-demethyl-2α-hydroxyhomolycorine, *O*-methyllycorenine, oduline, 6-*O*-methyloduline, dubiusine, 2*α*-hydroxy-6-*O*-methyloduline, 8-*O*-demethylhomolycorine-*N*-oxide, poetinatine

Structure type	Alkaloid name
Haemanthamine	vittatine, maritidine, *O*-methylmaritidine, 8-*O*-demethylmaritidine, 9-*O*-demethylmaritidine, crinamine, papyramine, 6-epipapyramine, *O*-methyl-6-epipapyramine, 6*α*-hydroxy-3-*O*-methylepimaritidine, 6*β*-hydroxy-3-*O*-methylepimaritidine, narcidine, haemanthamine, 11-*O*-acetylhaemanthamine, haemanthidine, 6-epihaemanthidine, cantabricine, narcimarkine, bujeine
Tazettine	tazettine, criwelline, pretazettine, 3-epimacronine, obesine
Narciclasine and montanine	narciclasine, narciprimine, trisphaeridine, bicolorine, ismine, pancracine, nangustine
Galanthamine	galanthamine, epigalanthamine, *O*-acetylgalanthamine, norgalanthamine, epinorgalanthamine, *N*-formylnorgalanthamine, narcisine, narwedine, lycoramine, norlycoramine, epinorlycoramine
Other types	*O*-methylnorbelladine, **cherylline**, pallidiflorine, mesembrenone, mesembrenol, mesembrine, seco-isopowellaminone

Focusing on *Narcissus poeticus*, studies were performed on different varieties and cultivars, as shown in **Table 3**. As evident, the alkaloid content is diverse, even within one species. However, it is worth noting that data are results of GC/MS analysis, which should not be considered entirely reliable but rather predictive. Therefore, the alkaloid content may differ after a phytochemical study involving isolation and structure evaluation by NMR analysis.

Except for wild varieties, there are plenty of cultivars of this plant. Because most *Narcissus* species can hybridize, it has become very popular to produce a large number of cultivars for ornamental purposes, with over 27,000 names of *Narcissus* cultivars now registered in the International Daffodil Register. The Amaryllidaceae cultivars have advantages for commercial alkaloid production.[13]

Table 3. *Occurrence of alkaloids in different varieties and cultivars of N. poeticus detected by GC/MS.*

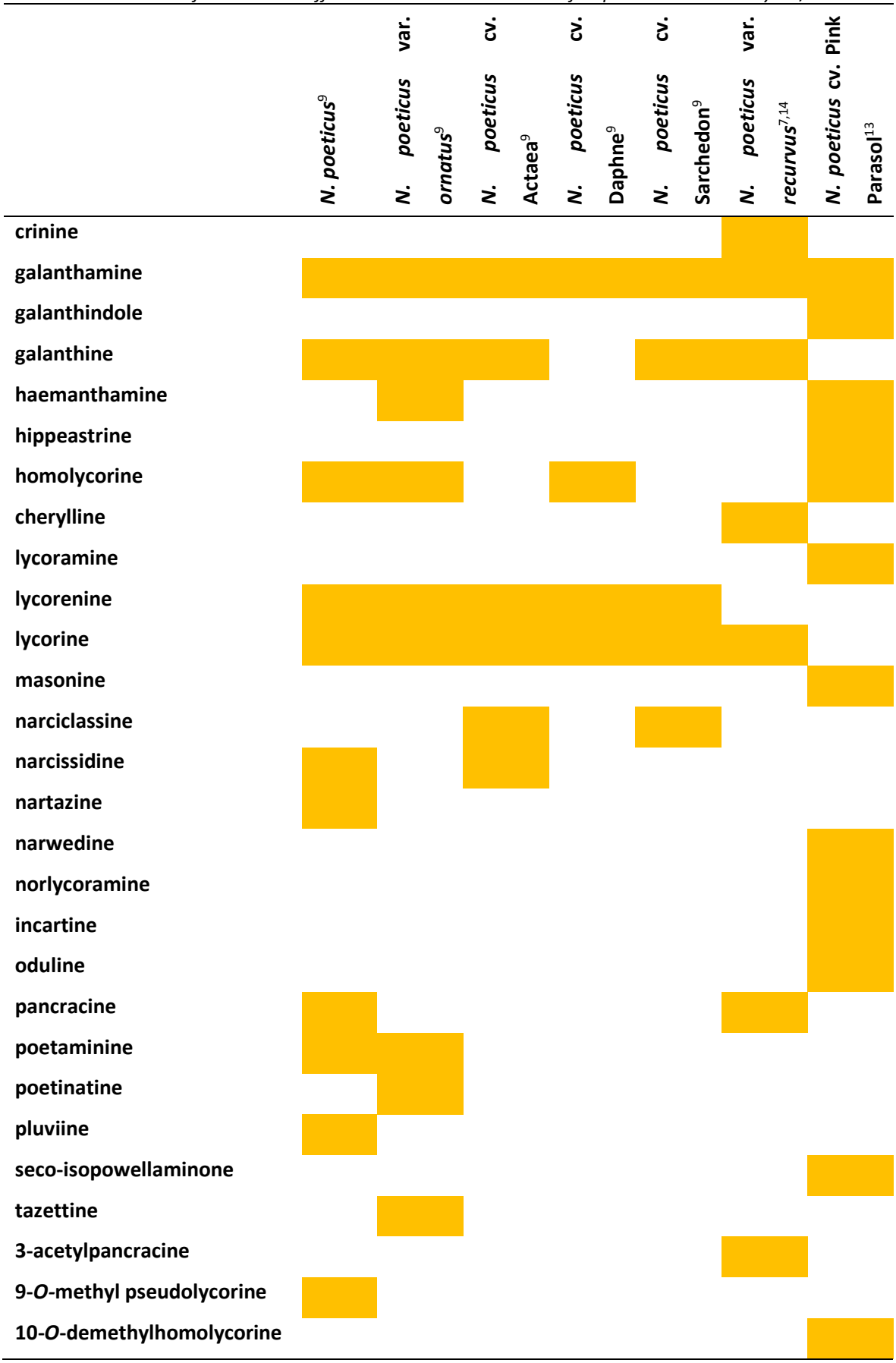

Some studies published not just the diversity of cultivars, which differs genetically and also environmentally (this has an impact on the final biosynthesis of alkaloids),[15] but also on different locations of alkaloids in the plant. A study by Torras-Claveria and co-workers compared the alkaloid profile in leaves and bulbs of different *Narcissus* cultivars by GC/MS analysis. Leaves were identified as having broader alkaloid content than the bulbs. In contrast, lycorine-type was the predominant alkaloid content of cultivar leaves, whereas the content of bulbs showed also galanthamine structural type.[16]

3.2.1 Galanthamine

From **Table 3** and also from the mentioned study which compared different *Narcissus* cultivars,[16] is certain that the most commonly found individual alkaloid was galanthamine.

Galanthamine AChE inhibiting properties had been demonstrated by Maskovsky and Kruglikova-Lvova in 1951, even before its first isolation from *Galanthus woronowii* in 1952. In the year 1956, suggestions for alternative sources of galanthamine including leaves of *Narcissus* spp. and *Galanthus nivalis,* as well as *Leucojum aestivum,* appeared. In the 1990s, the clinical development of galanthamine into a medication for AD started,[17] and in 2001 galanthamine was approved by the Food and Drug Administration (FDA) for the treatment of mild to moderately severe AD with the brand name Reminyl.[18]

The important source used for the isolation of galanthamine is the genus *Narcissus*,[19] but only certain varieties (etc. cv. Carlton) grown under specific conditions produce enough galanthamine to make it economically viable to extract for commercial purposes.[20] In recent years also other ways of obtaining galanthamine appeared, e.g., total synthesis of (−)-galanthamine[21,22] or *in vitro* production of galanthamine.[23]

Galanthamine, an Amaryllidaceae alkaloid with very good *h*AChE inhibitory activity, became the inspiration for testing all Amaryllidaceae alkaloids. To the best of our knowledge, about 214 of all known AAs and extracts from over 106 species have been tested for their ability to inhibit the AChE.[24]

3.3 Alzheimer's disease

AD can be defined as a progressive neurodegenerative disease characterized by cerebral neural loss leading to (among others) lack of acetylcholine (Ach) in the brain which causes typical syndrome of dementia with prominent progressive memory loss (as well as other cognitive abilities) and behavioral changes.[25]

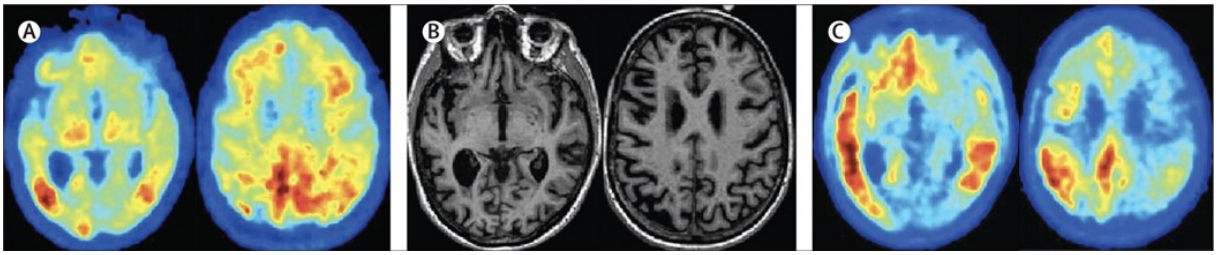

Figure 2. *Changes in the brain during AD. (A) Amyloid Pittsburgh compound B-PET scan showing amyloid deposition predominantly in the posterior cingulate region. (B) T1-weighted MRI images showing generalized cortical atrophy, left to right. (C) Tau-PET image using AV1451 tracer, showing left-sided inferotemporal lobe, parietal, and mild posterior cingulate deposition of tau.*[26]

AD accounts for approximately 60-70% of all dementia cases worldwide.[27] The prevalence of dementia increases with age. Approximately 5-8% are affected over the age of 65, and the number increases to 25-50% as the age rises over 85.[28] Age and presence of allele for apolipoprotein E4 are the most prominent risk factors, other risk factors include female gender, Down syndrome or AD in family history, cerebrovascular diseases, arterial hypertension and head injury in personal medical history.[25]

Histopathologically is AD characterized by accumulation of beta-amyloid (Aβ) (pathological form of amyloid precursor protein) in brain tissue and hyperphosphorylation of tau protein, causing formation of neurofibrillary tangles in cytoplasm of neurons (**Figure 3**).[29]

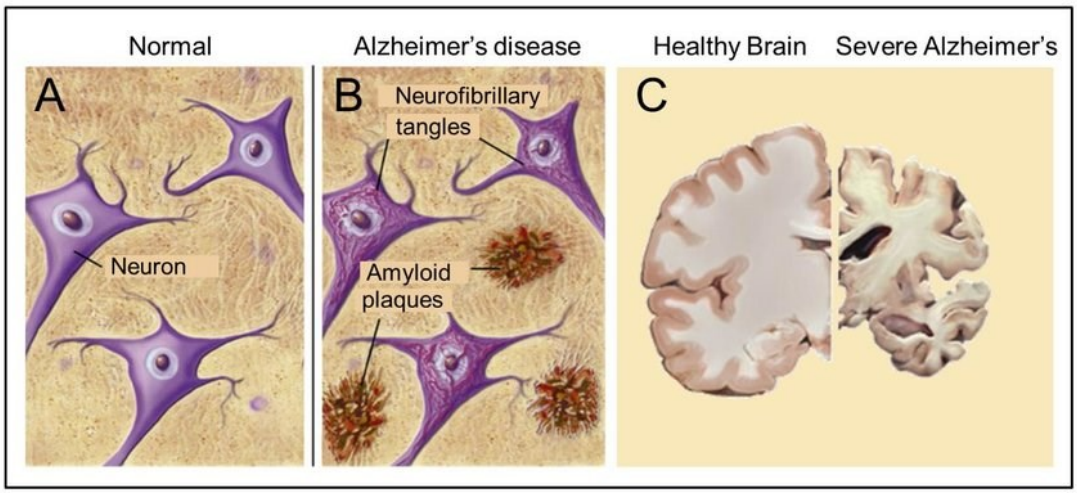

Figure 3. *Visualisation of histopathological changes in AD. Major pathological hallmarks of AD are amyloid plaques and neurofibrillary tangles (B) that are absent in healthy brain tissue (A). Massive apoptosis occurs in later stages of the development of AD in the human brain (brain slices) (C).*[30]

Currently, several hypotheses attempt to explain the impact of histopathological changes on neurons, while the most prominent is the cholinergic hypothesis. Other hypotheses include e.g., neuroinflammation, oxidative stress, mitochondrial dysfunction, and vascular hypothesis.[25,27]

Clinical picture of AD is characterized by a global cognitive decline, which has progressive character and eventually leads to complete disruption of the patient's personality and loss of autonomy. AD is typically divided into three stages based on the severity of described symptoms.[25]

Clinical diagnosis is based on demonstration of dementia syndrome, defined by a progressive decline in at least two cognitive domains and a loss of patient autonomy. Diagnoses are confirmed by excluding other causes of dementia (e.g., systemic diseases, structural brain lesions). Various clinical tools (e.g. questionnaires, physical examinations) and paraclinical methods (e.g., biochemical blood profile, brain imaging such as computed tomography, magnetic resonance imaging, and positron emission tomography with fludeoxyglucose F18) are used in diagnostic process. In specific cases biomarkers in cerebrospinal fluid may be determined, following the ATN classification (amyloid/ tau/ neurodegeneration).[25,29]

Approved pharmacological treatments that encompass the standard of care for many patients with AD include cholinesterase inhibitors and the N-methyl-D-aspartate receptor (NMDA) antagonist memantine.[26] Interesting compound is huperzine A (from *Huperzia serrata*) with AChE inhibitory and NMDA antagonistic activity. It was approved by the FDA as a dietary ingredient, while in China it had been approved for the treatment of mild cognitive impairment in various doses and forms.[31] Recently FDA-approved anti-Aβ monoclonal antibodies are presented as drugs that may decrease the evolution of AD.[32] First, aducanumab (approved by the FDA in 2021 with the brand name Aduhelm) is selective for aggregated Aβ forms which results in reducing the brain burden of Aβ plaques.[33] It is worth noting that the European Medicines Agency (EMA) rejected the marketing authorisation application for aducunumab in 2021.[34] The second, lecanemab (approved by FDA in 2023 with the brand name Leqembi) decreases pathogenic Aβ, prevents Aβ deposition, and specifically diminish Aβ protofibrils in the brain.[35] EMA has not approved the drug until August 2024.[36]

3.3.1 Cholinergic hypothesis

A cholinergic hypothesis of AD was proposed due to the essential role of acetylcholine (Ach) in cognitive function. Ach is involved in several physiological processes such as memory, attention, sensory information, learning, and other critical functions. Ach is synthesized in the cytoplasm of cholinergic neurons from choline and acetyl-coenzyme A by the choline acetyltransferase enzyme (ChAT) and transported to the synaptic vesicles by vesicular acetylcholine transporter (**Figure 4**).[37]

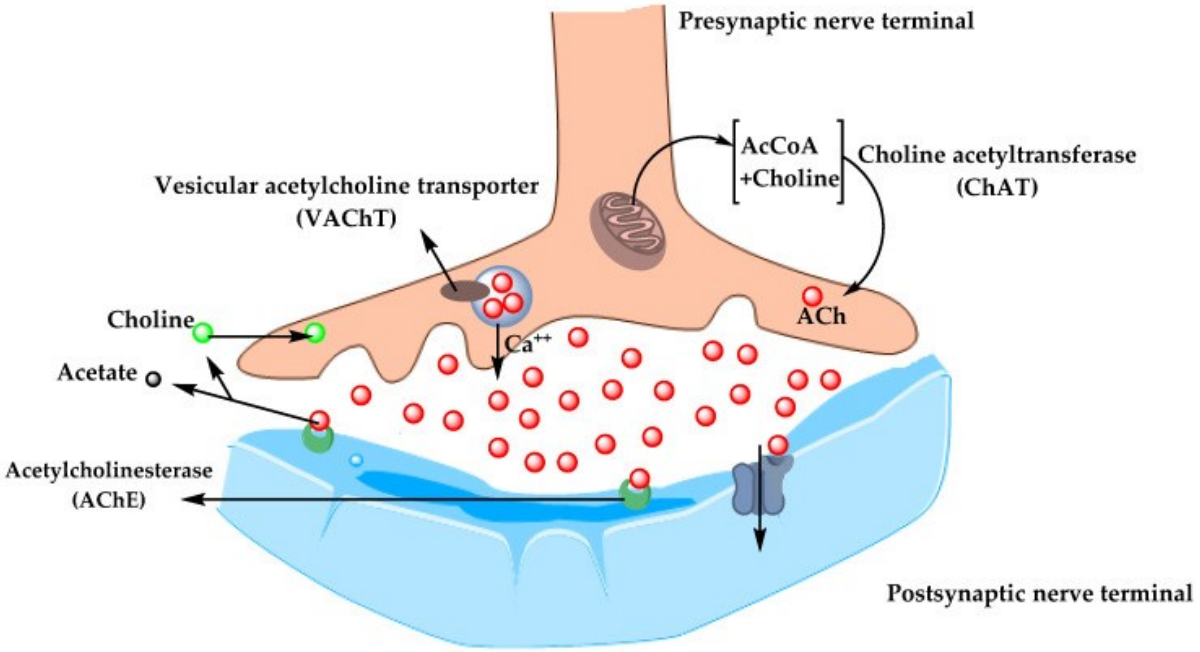

Figure 4. *The pathway for the synthesis and transportation of acetylcholine between presynaptic and postsynaptic nerve terminals.*[37]

Degeneration of the cholinergic neurons was found to take place in AD and to cause an alteration in cognitive function and memory loss. Aβ is believed to affect cholinergic neurotransmission and to cause a reduction in choline uptake and a release of ACh.[37] This fact is caused also by a reduction in cholinergic markers, such as ChAT.[27]

AChE is a serine-protease that plays a pivotal role in cholinergic transmission. The physiological function of AChE is to hydrolyse ACh to afford choline and acetic acid.[38] AChE is mainly expressed in nervous tissue, neuromuscular junctions, plasma, and red blood cells.[39] In the human brain, there are two structural types of AChE: type G4 (tetramer, highly prevalent) and monomer G1 (in minor amounts). The proportion of G1 is significantly increased in AD.[40]

Another cholinesterase, butyrylcholinesterase (BuChE), can also inactivate ACh. Whilst, under normal conditions, BuChE is responsible for 20% of the total brain cholinesterase activity, in the later stages of AD, the activity of BuChE increases to 40–90% in certain brain regions.[40] Apart from its role in the cholinergic hypothesis, BuChE has been implicated in the deposition of amyloid.[41] Also, the interaction between AChE and PS-1, a key enzyme involved in Aβ production, was described. AChE binds directly to PS-1 to enhance its expression and subsequently increase the level of Aβ. It accelerates cognitive dysfunction in AD. Additionally, abnormal changes in the central cholinergic system can stimulate inflammation in nerve cells and the phosphorylation of Tau protein, thereby resulting in imbalanced neurotransmitters and neuronal apoptosis.[27]

For the broad effect of cholinesterases on AD, cholinesterase inhibitors (ChIs) are used for the symptomatic treatment of AD. Acetylcholinesterase inhibitors (AChEIs) are used to inhibit

acetylcholine degradation in the synapses, which results in continuous accumulation of ACh and activation of cholinergic receptors. Tacrine was the first FDA-approved ChI for the treatment of AD, but it exited the market because of hepatotoxicity side effects. Donepezil, rivastigmine, and galanthamine are currently in use for the symptomatic treatment of AD.[37] Interestingly, rivastigmine is a derivative of the natural compound physostigmine, which was studied as early AChEI, but it was poorly tolerated and had a short duration of action. In comparison, rivastigmine is represented with improved pharmacokinetic and stability profiles.[42] This leads to another important field of phytochemistry, the synthesis of semisynthetic or synthetic derivatives from natural compounds with improved properties.

As was already mentioned above, galanthamine and many other AAs were described for ChE inhibitory activity. Galanthamine, haemanthamine, lycorine and pancratistatin are lead molecules in AD and also anticancer drug research. Many novel hybrid derivatives, such as donepezil-tacrine, oxoisoaporphine-tacrine, galanthamine-curcumine, and other dual-site binding AChEI, exhibit a high AChE inhibitory activity with IC_{50} values in the nanomolar range, have been studied from a pharmacological and biochemical point of view or in mouse and rat models.[24]

3.3.2 Another targets for AAs

AAs are also tested for other AD targets. An important target is glycogen synthase kinase 3β (GSK-3β), which has been found to play a crucial role in neurodegeneration in general and AD in particular. In AD, the overactivity and/or overexpression of GSK-3β accounts for memory impairment, tau hyperphosphorylation, increased Aβ production, and local plaque-associated microglial-mediated inflammatory responses, which are hallmarks of the disease.[40]

Another interesting target of AAs is the enzyme prolyl oligopeptidase (POP). It has been discussed that reduced POP activity correlated to the tau pathology and severity of AD.[40]

3.4 Anticancer activity of AAs

The potency of several AAs against the emergence of some solid tumours was recently reviewed, highlighting the various mechanisms that have been invoked to explain the cytotoxic effects of AAs.[43]

This master's thesis focuses primarily on the alkaloid lycorine, which is described in detail below. Other AAs with notable anticancer activity are also briefly reviewed.

3.4.1 Lycorine

A landmark achievement in the field was the isolation of lycorine from *Narcissus pseudonarcissus* in 1877 as the first alkaloid of the Amaryllidaceae, followed by its structure elucidation several decades later in 1956. [44] Lycorine does not occur just in *Narcissus* sp., other species also contain this alkaloid, including *Lycoris radiata, Leucojum aestivum, Hymenocallis littoralis, Hippeastrum equestre,* flowers of *Clivia nobilis, Ammocharis coranica, Brusvigia radulosa, Crinum macowanii.*[45]

The antiproliferative effects of lycorine in several cancer cell lines have been known since the 1920s.[44] **Table 4** shows an overview of lycorine's broad anticancer activity.

Table 4*. Anticancer activity of lycorine in different cancer cell lines*

Tumour type	Cell line	IC_{50} [µM]	Reference
leukaemia	HL-60	1.0 ± 0.0	[46]
	K562	3.6 ± 1.2	[46]
	U937	2.4 ± 0.0	[46]
	CEM	1.6 ± 0.0	[46]
multiple myeloma	KM3	1.3 ± 0.0	[46]
glioblastoma	Hs683	6.9 ± 0.5	[46]
	U373	7.6 ± 0.2	[47]
	T98G	3.0[4]	[4]
	C-6	<10	[48]
melanoma	SKMEL-28	8.5 ± 0.3	[46]
	B16F10	6.3 ± 0.2	[46]
breast adenocarcinoma	MCF-7	13.0 ± 2.9	[46]
ovarian carcinoma	Hey1B	1.2 ± 0.0	[46]
	SK-OV-3	3.0 ± 0.3	[49]
	CHO-K1	<10	[48]

Tumour type	Cell line	IC_{50} [μM]	Reference
prostatic adenocarcinoma	PC-3M	2∼5	[45]
colon carcinoma	HT-29	3.2 ± 0.0	[46]
	HepG2	3.7 ± 0.0	[46]
	HCT116	3.0 ± 0.2	[49]
	COL-2	0.4 (ED_{50})	[50]
hepatoma	G-361	5.0 ± 0.3	[46]
	C8161	1.2 ± 0.0	[46]
esophageal carcinoma	OE21	4.5 ± 0.7	[46]
	BJ	1.9 ± 0.1	[46]
cervical adenocarcinoma	Hela	10.6 ± 0.9	[46]
human bladder carcinoma	T24	7.5	[45]
lung cancer	A549	4.2 ± 0.4	[46]
	LLC	0.5 ± 0.0	[46]
	NCI-H460	3.3 ± 0.3	[49]

Although there is no specific mechanism of action for lycorine, it is a candidate anticancer drug. Various biological mechanisms were described for lycorine to explain its anticancer activity.[51] On promyelocytic leukaemia, lycorine is capable of arresting the cell cycle at the G2/M phase at 5 μM concentration. It was also found that exposure to lycorine with the same concentration can induce apoptosis of leukaemia cells via activation of caspases.[52] Lycorine interferes with vitamin C biosynthesis and also proved to be able to interact with DNA or inhibit cell proliferation and induce apoptosis.[51] Another study described lycorine as a potent NF-κB signalling pathway inhibitor in prostate cancer.[53]

Several structural features for the anti-tumour activity of lycorine were found. The presence of the unaltered hydroxyl groups at the C-1 and C-2 positions in their original form is essential for the anti-tumour property. There is an absolute requirement for the presence of basic nitrogen at position N-6 of the B-ring. Quaternization by incorporation of methyl iodide or amide to this nitrogen resulted in a loss of activity. Another structural feature is the stereochemistry and conformational freedom of the C-ring. Other features that might provide useful guidelines for future analogue design are lipophilicity and conjugation of long-chain fatty acids.[45] This structure-activity relationship can be applied to lycorine structure-type alkaloids and their derivatives.

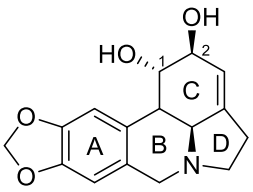

Figure 5. *Structure of lycorine.*

From lycorine structure type and derivatives good anticancer activity was described for amarbellisine and ungeremine.[52]

3.4.2 Haemanthamine structure type

Haemanthamine displays significant cytotoxic activity against several different types of cancer cell lines, including MOLT-4, HepG2, HeLa, MCF-7, CEM, K562, A549, Caco-2, HT-29, A2780, SW1573 and T47-D.[52]

One of the mechanisms of action is binding to the peptidyl transferase centre of the eukaryotic ribosome and thus inhibits protein synthesis.[54] Another mechanism of action is increasing cell apoptosis and activation of caspases 3, 7, 8, and 9, decreasing mitochondrial membrane potential and arresting the cell cycle in the G1 and G2/M phase.[52]

There was the first universal LC-MS/MS method for quantification of haemanthamine in rat plasma, bile, and urine determined by Hroch and co-workers demonstrated excessive distribution to tissues and rapid excretion, primarily into the urine.[55]

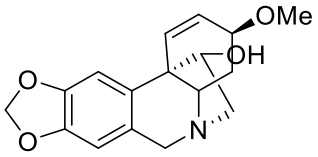

Figure 6. *Structure of haemanthamine.*

Haemanthidine was also described for its promising anticancer activity against A549, OE21, Hs683, and SKMEL cancer cells.[52]

Several derivatives of haemanthamine and haemanthidine were prepared, while some had promising anticancer activity against human solid tumour cells.[56] An important role in the activity is connected to the methoxy group at C-3, together with a hydroxyl group at C-11.[54]

3.4.3 Narciclasine and montanine structure type

Narciclasine demonstrated potent anti-tumour effects in a screen involving six different human cancers (mean IC_{50} 0.03 µM), including apoptosis-sensitive (MCF-7, PC-3) and apoptosis-resistant (A549, U373) cells.[57]

Mechanism studies showed that narciclasine could interact with the ribosomal 60s subunit and inhibit the formation of peptide bonds. Another study reported that this alkaloid induced apoptosis by affecting the AMPK-ULK1 signalling pathway in triple-negative breast cancer cell lines. Interestingly, narciclasine inhibited Topoisomerase I (Topo I) activity but had no obvious effect on Topoisomerase II (Topo II).[58]

A study by Ingrassia and co-workers found that almost none of the chemical modifications to narciclasine improved antiproliferative IC_{50} values. Only esters of the hydroxyl at position R1 possibly improved the in vitro anti-tumour activity of narciclasine.[59]

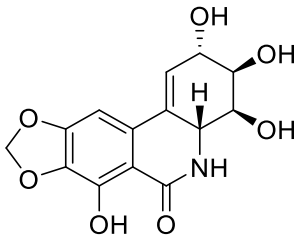

Figure 7. *Structure of narciclasine.*

Pancratistatin exhibited submicromolar (grow inhibition 50% (GI_{50}) = 0.091 µM) activities in cancer cell line screening.[58] Pancratistatin and its derivatives disrupted mitochondrial function and activated the intrinsic apoptotic pathway.[60]

Montanine demonstrated a strong antiproliferative and cytotoxic effect on cancer cell lines, including MCF-7, Hs578T, MDA-MB-231, HCT-15, A549, and SK-MEL-28. Interestingly, montanine-type alkaloids can be easily obtained from alkaloids with a haemanthamine skeleton, which is more common and available from Amaryllidaceae plants.[61]

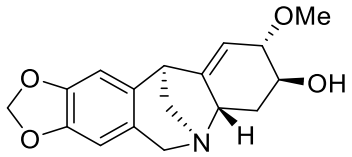

Figure 8. *Structure of montanine.*

4 Experimental section

4.1 Materials

4.1.1 Chemicals for extraction, isolation, and structure evaluation of alkaloids

- Acetic acid 1% (CH_3COOH) (Ing. Petr Švec – Penta, Prague)
- Acetonitrile (ACN) (Ing. Petr Švec – Penta, Prague)
- Acetonitrile HPLC gradient (ACN) (Lach-Ner, Neratovice)
- Ammonium hydroxide solution (NH_4OH), 28-30% NH_3 in water (Ing. Petr Švec – Penta, Prague)
- Benzine (Ing. Petr Švec – Penta, Prague)
- Chloroform ($CHCl_3$) (Ing. Petr Švec – Penta, Prague)
- Chloroform-*d* 99.8 atom% D ($CDCl_3$) (Sigma-Aldrich, Prague)
- Distilled water
- Dichloromethane (CH_2Cl_2) (Ing. Petr Švec – Penta, Prague)
- Diethyl amine (DEA) (Ing. Petr Švec – Penta, Prague)
- Diethyl ether (Et_2O) (Ing. Petr Švec – Penta, Prague)
- Dimethyl sulfoxide (DMSO)
- Dimethyl sulfoxide-d_6 99.5 atom% ($(CD_3)_2SO$) (Sigma-Aldrich, Prague)
- Dragendorff's reagent (laboratory preparation)[62]
- Ethanol 96% (EtOH) (Ing. Petr Švec – Penta, Prague)
- Ethyl acetate (EtOAc) (Ing. Petr Švec – Penta, Prague)
- Ethanol HPLC gradient (EtOH) (VWR International, France)
- Formic acid LC-MS quality (HCOOH) (VWR Chemicals, Stříbrná Skalice)
- Hydrochloric acid 2% (HCl) (Ing. Petr Švec – Penta, Prague)
- Mayer's reagent (laboratory preparation)[63]
- Methanol (MeOH) (Ing. Petr Švec – Penta, Prague)
- Methanol HPLC gradient (MeOH) (VWR International, France)
- Methanol LC-MS CHROMASOLV (MeOH) (Sigma-Aldrich, Prague)
- Methanol-d_4 99 atom% D (CD_3OD) (Sigma-Aldrich, Prague)
- Sodium carbonate 10% (Na_2CO_3) (Ing. Petr Švec – Penta, Prague)
- Sodium sulphate anhydrous (Na_2SO_4) (Ing. Petr Švec – Penta, Prague)
- Toluene (To) (Ing. Petr Švec – Penta, Prague)

4.1.2 Materials for measuring biological activity

4.1.2.1 Chemicals and enzymes for measuring inhibitory activity against *h*AChE and *h*BuChE

- 5,5'-Dithio-bis-(2-nitrobenzoic) acid (DTNB), Ellman's Reagent (Sigma-Aldrich, Prague)
- Acetylthiocholine iodide (AcTCh) (Sigma-Aldrich, Prague)
- Butyrylthiocholine iodide (BuTCh) (Sigma-Aldrich, Prague)
- Dimethyl sulfoxide p.a. (DMSO) (Sigma-Aldrich, Germany)
- Eserine (Sigma-Aldrich, Prague)
- Galanthamine hydrobromide (Sigma-Aldrich, Prague)
- Human recombinant acetylcholinesterase (*h*AChE) (Department of Chemistry, Faculty of Science, University of Hradec Králové)
- Human recombinant butyrylcholinesterase (*h*BuChE) (Department of Chemistry, Faculty of Science, University of Hradec Králové)
- Phosphate buffer (pH 7.4) (laboratory preparation)

4.1.2.2 Cell culture and chemicals for cytotoxicity screening

Cytotoxicity assay determined at the Faculty of Medicine in Hradec Králové, Charles University:

- Jurkat (acute T-cell leukaemia)
- MOLT-4 (acute lymphoblastic leukaemia)
- A549 (lung carcinoma)
- HT-29 (colorectal adenocarcinoma)
- PANC-1 (pancreas epithelioid carcinoma)
- A2780 (ovarian carcinoma)
- SHSY5Y (human neuroblastoma)
- MCF-7 (breast adenocarcinoma)
- SAOS-2 (osteosarcoma)
- MRC-5 (non-tumour lung fibroblasts)
- Doxorubicin 1 µM (positive control) (Sigma-Aldrich, St. Louis, USA)

Selected human tumour and non-tumour cell lines were purchased from the European Collection of Authenticated Cell Cultures (ECACC, Salisbury, UK).

Cytotoxicity assay determined at Faculty of Pharmacy, University of Ljubljana:

- CellTiter96 Aqueous One Solution Reagent (10 µL; Promega, Madison, WI, USA)
- Dubecco's modified Eagle's medium (Sigma-Aldrich, St. Louis, MO, USA)
- Fetal bovine serum (Gibco, Thermo Fisher Scientific, Waltham, MA, USA)
- 2 mM l-glutamine (Sigma-Aldrich, St. Louis, MO, USA)

- 100 U/mL penicillin (Sigma-Aldrich, St. Louis, MO, USA)
- 100 µg/mL streptomycin (Sigma-Aldrich, St. Louis, MO, USA)

The MCF-7 cell line was obtained from the American Type Culture Collection (ATCC, Manassas, VA, USA).

4.1.2.3 Enzymes and chemicals for measuring the inhibitory activity of human topoisomerase IIα

- 0.008% Tween
- 0.008% Tween with 10% DMSO
- Adenosine triphosphate (ATP)
- Assay Buffer
- Dilution Buffer
- Human topoisomerase IIα (Topo IIα)
- T10 Buffer
- Transposon from *Fusarium oxysporum* (TFO1, oligonucleotide)
- Triplex Formation Buffer (TF Buffer)
- Wash Buffer

Enzymes and chemicals were utilized at the Department of Pharmaceutical Chemistry, Faculty of Pharmacy, University of Ljubljana; however, the sources of these materials were not specified.

4.1.2.4 Stems used for antibacterial and antifungal activity

Antibacterial:

- SA – *Staphylococcus aureus* subsp. *aureus*
- MRSA – *Staphylococcus aureus* subsp. *aureus*
- SE – *Staphylococcus epidermalis*
- EF – *Enterococcus faecalis*
- EC – *Escherichia coli*
- KO – *Klebsiella pneumoniae*
- ACI – *Acinetobacter baumannii*
- PA – *Pseudomonas aeruginosa*

Antifungal:

- CA1 – *Candida albicans*
- CK – *Candida krusei*
- CP – *Candida parapsilosis*
- CT – *Candida tropicalis*

- AF – *Aspergillus fumigatus*
- AFla – *Aspergillus flavus*
- AC – *Absidia corymbifera*
- TI – *Trichophyton inerdigitale*

4.1.3 Auxiliary materials for extraction, separation, and isolation

- Commercial chromatographic plates, 20 × 20 cm, 0.2 mm thick, coated with silica gel 60 GF_{254} (Merck, Germany)
- Glass plates 150 x 150 mm with silica gel Kieselgel 60 GF_{254} (Merck, Germany) (laboratory preparation)
- Silica gel 40–63 µm (SiO_2) (Merck, Germany)
- Silica gel Kieselgel 60 GF_{254} (Merck, Germany)

4.1.4 Instrumentation

- Flash Chromatography System BÜCHI Sepacore Flash System X10 (BÜCHI, Switzerland)
- GEMO Fritz-Muller D-74653 Ingelfingen Valve Pump (GEMÜ Gebrüder Müller, Germany)
- Microplate reader (Synergy 4 Hybrid; BioTek, Winooski, VT, USA)
- MS-EI Spectrometer on GC/MS System Agilent 7890A GC 5975 Inert MSD; EI Mode 70 eV; Column HP-5 MS (30 m × 0.25 mm × 0.25 µm) (Agilent Technologies, Santa Clara, California, USA)
- MS-ESI Spectrometer Waters Acquity qDa and Diode Array Detector Waters 2998 on HPLC System Waters Autopurification™ (Milford, USA)
- Polarimeter P3000 (A. Krüss Optronic, Hamburg, Germany)
- Rotary Vacuum Evaporator for Pilot Scale Use (Laborota 20 Heidolph, Germany)
- Spectrometer Varian VNMR S500 (Varian, Palo Alto, California, USA)
- Ultrasonic Water Bath Sonorex Super 10P (Bandelin, Germany)
- UV Reader Synergy HT (Biotek, USA)
- Vacuum Evaporator Büchi Rotavapor R-114 (Büchi Labortechnik AG, Switzerland)

4.1.5 Plant material

The plant material for our work consisted of 29 kg of fresh bulbs of *Narcissus poeticus* var. *recurvus*, purchased from Lukon Glads s.r.o., Lysá nad Labem. The botanical identification was carried out by Prof. RNDr. Lubomír Opletal, CSc. A voucher specimen is deposited in the Herbarium of the Faculty of Pharmacy in Hradec Králové under number CUFP-16130/AL-748.

4.2 Methods

4.2.1 Isolation methods

In the isolation of alkaloids, a range of methodologies was applied, including:

- **Flash chromatography**
    - Performed by gradient elution on a stationary phase consisting of SiO_2. The adsorbent-solvent mixture was poured onto the chromatographic column in the usual manner. The tested sample was applied to the column in the form of trituration with an adsorbent. This method was carried out at the Department of Pharmacognosy and Pharmaceutical Botany, Faculty of Pharmacy in Hradec Králové, Charles University, with the assistance of Assoc. Prof. PharmDr. Jakub Chlebek, Ph.D.
- **TLC method (analytical and preparative)**
    - Performed using commercial chromatographic plates (10 × 20 cm, 0.2 mm thick) or glass plates (150 × 150 mm) with silica gel. The plates were developed in the chromatographic chambers saturated with experimentally determined mobile phases (MP). Developed plates were dried and detected using a UV [λ = 254 nm], followed by detection with spray Dragendorff's reagent.
- **Recrystallization**
    - The recrystallisation method was used for the separation and purification of some alkaloids. This process was based on using two different solvents with different polarity and substance solubility.

A detailed description of the alkaloid isolation process is provided below in section **4.3.**

4.2.2 Methods for structural analysis

The chemical structures were elucidated by a combination of mass spectrometry (MS), one-dimensional (1D), and two-dimensional (2D) nuclear magnetic resonance (NMR) spectroscopic techniques, optical rotation, and by comparison with literature data.

4.2.2.1 GC/MS-EI analytical method

Analysis by GC/MS was performed with the assistance of RNDr. Jaroslav Jenčo, Ph.D. at the Department of Pharmacognosy and Pharmaceutical Botany.

Samples for analysis (0.2–0.5 mg) were dissolved in 1 mL of LC/MS-grade MeOH and measured using an Agilent 7890A GC 5975 gas chromatograph with an HP-5 column. A volume of 1 µL of the analysed sample was applied to the column (HP-5; 30 m × 0.25 mm × 0.25 µm, Agilent Technologies, Santa Clara, CA, USA) with a split ratio of 1:10 at a temperature of 280 °C. The following temperature gradient was used for the analysis: the temperature increased from 100 °C to 180 °C at a rate of 15 °C/min. Then, the temperature was stabilized at 180 °C for one minute. After that, the temperature increased from 180 °C to 300 °C at a rate of 5 °C/min, followed by stabilization at 300 °C for fifteen minutes. Helium was used as the carrier gas with a flow rate of 0.8 mL/min. Detection was performed using a mass spectrometer with electron ionization at 70 eV.

The results of the alkaloid analyses were compared with the NIST 11 spectrum library (National Institute of Standards and Technology Library, USA). This comparison enabled the prediction of alkaloid structures based on the mass spectrum obtained from the sample.

4.2.2.2 HPLC/MS-ESI analytical method

Analysis by HPLC/MS was performed with the assistance of RNDr. Jaroslav Jenčo, Ph.D. at the Department of Pharmacognosy and Pharmaceutical Botany, Faculty of Pharmacy in Hradec Králové, Charles University.

Samples for analysis (0.2–0.3 mg) were dissolved in 1 mL of LC/MS-grade MeOH and measured using the Waters Autopurification™ HPLC/MS system. The samples were analysed at room temperature. For separation, a reverse-phase column XSelect® CSH™ C18 OBD™ (100 mm × 4.6 mm, 5 µm) was used. The mobile phases consisted of water with 0.1% formic acid (solvent A) and methanol with 0.1% formic acid (solvent B), with a mobile phase flow rate of 1 mL/min.

The elution program with a gradient was as follows (v/v): 0 min 5% B, 5 min 100% B, 8.5 min 5% B, followed by 1.5 min under initial conditions for equilibration.

HPLC/MS mass spectra were recorded in the range of 200 to 800 m/z. The PDA detector range was set from λ = 190 to λ = 700 nm. HPLC/MS-ESI analyses were performed in positive ion mode.

This method was used to determine the molecular weight (MW) of alkaloids.

4.2.2.3 NMR analysis

Analysis by NMR spectroscopy was performed by my consultant PharmDr. Jana Křoustková, Ph.D. and by Assoc. Prof. PharmDr. Jiří Kuneš, CSc. at the Department of Organic and Bioorganic chemistry, Faculty of Pharmacy in Hradec Králové, Charles University.

Samples (1–5 mg) were dissolved in $CDCl_3$/CD_3OD/$(CD_3)_2SO$ (according to their solubility), and their NMR spectra were measured using a VNMR S500 instrument with a magnetic field frequency of 499.87 MHz (for ^1H nuclei) and 125.70 MHz (for ^{13}C nuclei). A broadband dual-channel gradient probe with temperature control (Varian OneNMR probe) was used for irradiation and signal detection. The chemical shift values were measured as δ ppm (parts per million) and were indirectly referenced to the tetramethylsilane standard using the residual solvent signal.

The chemical shifts values for solvents:

- **$CDCl_3$:** 7.26 ppm for a residual solvent ^1H signal; 77.0 ppm for a solvent ^{13}C signal
- **CD_3OD:** 3.31 ppm for a residual solvent ^1H signal; 49.0 ppm for a solvent ^{13}C signal
- **$(CD_3)_2SO$:** 2.50 ppm for a residual solvent ^1H signal; 39.7 ppm for a solvent ^{13}C signal

4.2.2.4 Optical rotation

Optical rotation was measured using a polarimeter. Samples were dissolved in $CHCl_3$ or a 1:1 mixture of $CHCl_3$ and EtOH at a concentration of 0.05–0.10 g/100 mL and measured at 21–22 °C, with five measurements taken per sample. The optical rotation was calculated from the average value according to the following formula:

$$[\alpha]_t^D = \frac{c \times l}{100 \times \alpha}$$

where:

α = optical rotation of the sample (°)

t = temperature of measurement (°C)

D = wavelength of the sodium D-line light (nm)

c = concentration of the sample in solution (g/100 mL)

l = path length of the cell (dm)

4.2.3 Methods for screening of biological activities

4.2.3.1 Determination of inhibitory activity against *h*AChE and *h*BuChE

Determination of inhibitory activity against *h*AChE and *h*BuChE was performed by PharmDr. Daniela Suchánková, Ph.D. at the Department of Pharmacognosy and Pharmaceutical Botany, Faculty of Pharmacy in Hradec Králové, Charles University.

Reagents for determining inhibitory activity against *h*AChE and *h*BuChE

- 5 mM DTNB solution in buffer
- 10 mM ATChI water solution
- 10 mM BuTChI water solution
- 100 mM phosphate buffer (pH 7.4)

Enzymes

The enzymes were prepared using recombinant technology at the Department of Chemistry, Faculty of Science, University of Hradec Králové.[64] A medium containing the enzymes was diluted with 100 mM phosphate buffer (pH 7.4) as needed to achieve an absorbance value of 0.08–0.15 for AChE and 0.15–0.20 for BuChE. The medium was aliquoted according to the required amount (calculated for subsequent dilution for measurement) into Eppendorf tubes, frozen, and stored in a freezer at −22 °C until use.

Determination of inhibitory activity of isolated alkaloids

The inhibitory activity of the substances was determined using **Ellman's spectrophotometric method**[65] with DTNB [λ = 412 nm]. Enzyme activity was determined by measuring the increase in absorbance at 37 °C at minute intervals using a Microplate Reader. The sample of a given concentration was always measured three times. The measured data were used to calculate the percent inhibition (%I) according to the formula:

$$\% I = 100 - \left(100 \times \frac{\Delta ABL}{\Delta ASA}\right)$$

% I – percentage of inhibition; ΔABL – decrease in absorbance of the blank sample over 1 minute; ΔASA – absorbance of the tested sample over 1 minute.

The results were compared with the IC_{50} values of known cholinesterase inhibitors – galanthamine (IC_{50} (*h*AChE) = 1.710 ± 0.065 μM, IC_{50} (*h*BuChE) = 42,301 ± 0,065 μM) and eserine (IC_{50} (*h*AChE) = 0.20 ± 0.01 μM; IC_{50} (*h*BuChE) = 0.30 ± 0.01 μM).

Measurement procedure

Into six wells of a microtiter plate, 8.3 µL of solution of the enzyme (AchE or BuChE) was pipetted, followed by the addition of 283 µL of 5 mM DTNB and 8.3 µL of solution of a sample, and the last row was pipetted with DMSO (instead of the test substance) as a blank sample. The mixture was stirred on a micro shaker for 1 minute and then incubated in the reader chamber at 37 °C for 5 minutes. After incubation, 33.3 µL of substrate solution (10 mM ATChI or 10 mM BuTChI) was added and then incubated in the reader chamber at 37 °C for 2 minutes. Absorbance was measured at the appropriate wavelength (412 nm). The difference was calculated as described above, and the average inhibition value with standard deviation was determined.

Initially, screening measurements were performed where all substances were tested at a concentration of 4 mM (out concentration) and 100 µM (in concentration). For substances that show an inhibitory potential greater than 50% at these concentrations, the IC_{50} was determined. IC_{50} values were calculated from the obtained values of AChE or BuChE activity reduction using nonlinear regression in GraphPad Prism software (Windows version 6.07; GraphPad Software, San Diego, CA, USA).

4.2.3.2 Determination of cytotoxic activity

Determination of cytotoxic activity was conducted in collaboration with the Department of Medical Biochemistry, Faculty of Medicine in Hradec Králové, Charles University, using the xCELLigence system. The testing was performed by Assoc. Prof. RNDr. Radim Havelek, Ph.D.

All cell lines were maintained at 37 °C in a humidified 5% carbon dioxide (CO_2) and 95% air incubator. The cells in low passage number (non-tumour primary cell line MRC-5 was used for a maximum of 10 passages and cancer cell lines were used for a maximum of 20 passages) and in an exponential growth phase were used for this study.

Each cell line was seeded at a previously established optimal density (1.103 to 50.103 cells per well) in a 96-well plate (TPP, Trasadingen, Switzerland) and cells were allowed to settle overnight. During screening tests for cytotoxicity, cells were treated with alkaloids at a final concentration of 10 µM for 48 hours. Doxorubicin, at a concentration of 1 µM, was used as a positive control. At the end of the culture period, the WST-1 proliferation assay (Roche, Basel, Switzerland) was performed according to the manufacturer's protocol. The absorbance was determined using a Tecan Spark microplate reader (Tecan, Männedorf, Switzerland). Each value is the mean of three independent experiments and represents the percentage of the proliferation of control, non-treated cells (100%). The growth percent (GP) value as the mean of the proliferation decrease was calculated for each cell line and derivative tested.

4.2.3.3 Determination of cytotoxicity activity against the MCF-7 cell line

Determination of cytotoxic activity was conducted in collaboration with the Department of Pharmaceutical Chemistry, Faculty of Pharmacy, University of Ljubljana, during the Erasmus+ project. The MTS assay[66] was performed by Assistant MSc. Jaka Dernovšek.

MCF-7 cells were incubated in a 5% CO_2 atmosphere at 37 °C. The cells were plated in 96-well plates at a density of 2000 cells per well. Afterwards, the cells were incubated for 24 h and then treated with the final compounds, positive control (1 µM 17-dimethylaminoethylamino-17-demethoxygeldanamycin (17-DMAG)) or vehicle control (0.5% DMSO). After the 72 h incubation, CellTiter96 Aqueous One Solution Reagent (10 µL) was added to each well, and the cells were incubated for an additional 3 h. Then the absorbance was measured using a microplate reader.

Independent experiments were performed in triplicate. The statistically significant differences ($p < 0.05$) were calculated between the treated groups and DMSO, using two-tailed Welch's t-tests. The IC_{50} values were determined using GraphPad Prism 8.0 software (San Diego, CA, USA), and represent the concentration at which a compound produced a half-maximal response; these are given as means from the independent measurements.

During the control NMR analysis (**Figure 9**) of samples before performing the assay, lycorine (**1**) sample showed an impure spectrum (blue), after it was stored in a fridge for almost 2 years. Red signals correspond to pure **1** after purification.

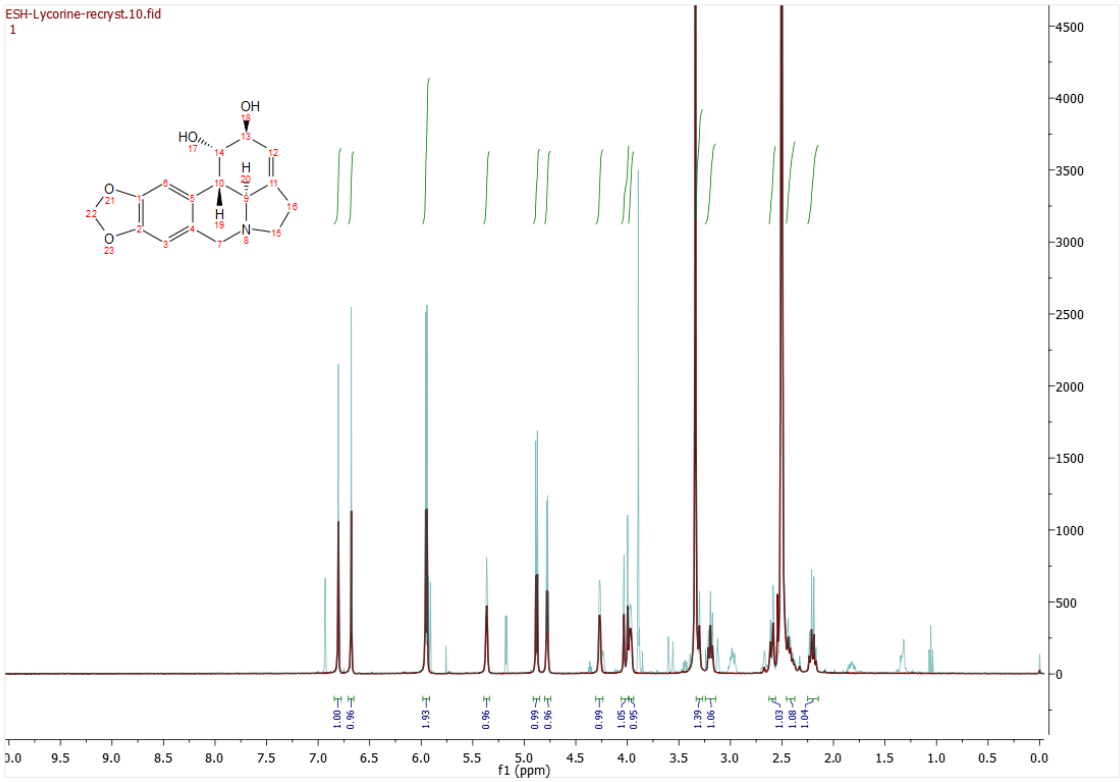

Figure 9. *Overlaid NMR spectra of pure (red) and impure **1** (blue).*

The purification process of **1** (**Figure 10**) has been investigated. 100 mg of the compound was dissolved in 5 mL of DMSO. Afterwards, the DMSO was evaporated by a rotavapor with an oil pump. Subsequently, the yield was dissolved in 300 µL of DMSO, leading to the formation of crystals. These crystals were collected by vacuum filtration and washed with MeOH. Finally, they were dried under a vacuum.

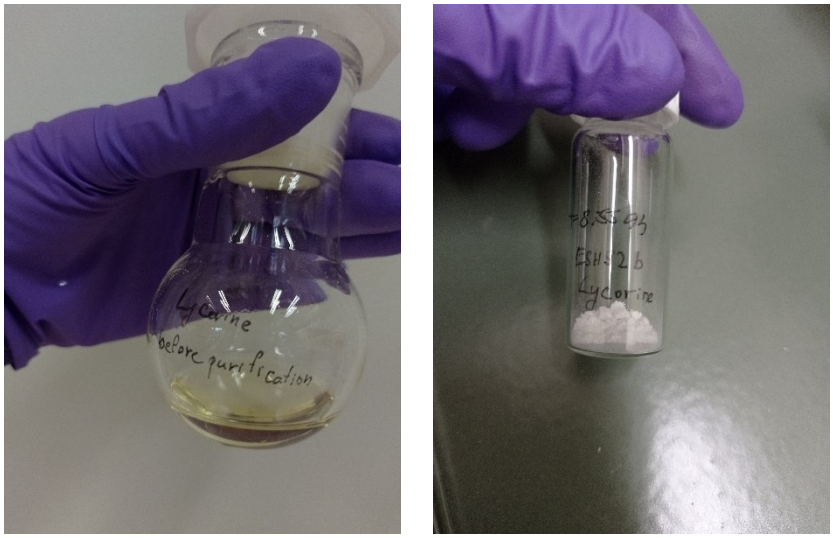

Figure 10. *Solution of **1** in DMSO before purification (left), pure compound (right).*

4.2.3.4 Determination of inhibitory activity against human topoisomerase IIα

Determination of inhibitory activity against human Topo IIα was conducted in collaboration with the Department of Pharmaceutical Chemistry, Faculty of Pharmacy, University of Ljubljana, during the Erasmus+ project. The testing was performed by MSc. Ana Jug.

For the enzyme incubation with the substrate, a mixture was prepared by combining Assay Buffer, ATP, water, and pNO1, which was added to each well, followed by the addition of an inhibitor to each well. The enzyme was then prepared by diluting Topo IIα with Dilution Buffer. The enzyme solution was added to each well, while the blank control was Dilution Buffer instead of the enzyme. The contents were mixed by pipetting and incubated for 30 minutes at 37°C.

TF Buffer was added to the wells, mixed by pipetting, and incubated for 30 minutes at room temperature. The dye mixture was added to each well, incubated for 15 minutes at room temperature in the dark, and mixed by pipetting.

The measurement of fluorescence was conducted using the BioTek® Synergy HT reader, with an excitation wavelength of 495 nm and an emission wavelength of 537 nm.

As standard was used N^6-(*tert*-butyl)-8-ethyl-N^2-(2-(2-morpholinoethoxy)quinoline-6-yl)-7*H*-purine-2,6-diamine, known, potent ATP-competitive inhibitor of Topo IIα from *Novartis* with $IC_{50} = 0.73 \pm 0.03$ µM.

4.2.3.5 Determination of antibacterial activity

Beyond the primary aims of this master's thesis, antibacterial activity was also evaluated at the Department of Biological and Medicinal Sciences, Faculty of Pharmacy in Hradec Králové, Charles University by Ida Dufková.

The microdilution broth method was applied to eight different bacterial strains, using Mueller-Hinton broth number 2 at pH 7.0, with incubation at 35 °C ± 2 °C for 24–48 hours. The results were determined visually using the AlamarBlue indicator.

4.2.3.6 Determination of antifungal activity

In addition to the primary aims of this master's thesis, antifungal activity was also evaluated at the Department of Biological and Medicinal Sciences, Faculty of Pharmacy in Hradec Králové, Charles University by Ida Dufková.

The microdilution broth method was applied to eight different fungal strains. RPMI 1640 medium with glutamine and 2% glucose was used, with a buffer at pH 7.0. The incubation was carried out at 35 °C ± 2 °C (TI 25–28 °C) for 24–48 hours (TI 5–7 days). The results were determined visually using the AlamarBlue indicator.

4.2.4 Methodology of molecular docking of isolated Amaryllidaceae alkaloids and semisynthetic derivatives of galanthine into *h*AChE

Inhibition of *h*AChE was tested not only by *in vitro* methods but also by *in silico* methods. For the purposes of this thesis, molecular docking, one of the most employed methods of the Structure-Based Drug Design (SBDD), was chosen. Molecular docking was conducted using the MOE (Molecular Operating Environment, v2022.02, Chemical Computing Group Inc., Montreal, QC, Canada) with the Amber10:EHT force field.

4.2.4.1 Enzyme preparation

The target of the molecular docking was the enzyme *h*AChE in complex with galanthamine, retrieved from the Protein Data Bank (PDB), available at https://www.rcsb.org/. This complex was selected due to the structural correlation of the co-crystallized ligand with our ligands, which are Amaryllidaceae alkaloids.

Characterization of the enzyme:

- **PBD ID:** 4EY6
- **PBD DOI:** 10.2210/pdb4EY6/pdb
- **Title:** Crystal Structure of Recombinant Human Acetylcholinesterase in Complex with (–)-galanthamine
- **Organism:** *Homo sapiens*
- **Resolution:** 2.40 Å
- **R-Value Free:** 0.208
- **R-Value Work:** 0.167
- **Number of subunits** = 2 (100% homodimer, subunit A was selected)

Before docking, the enzyme was prepared by removing subunit B, errors, water molecules, and excessive ligands (3,6,9,12,15,18,21-heptaoxatricosan-1,23-diol, 1,2-ethanediol, nitrate ion, 2-acetamido-2-deoxy-beta-*D*-glucopyranose). Subsequently, protonation and restrained energy minimization were performed. The ligand was then defined in the prepared structure of the enzyme.

To validate the chosen molecular docking algorithm, redocking of the original ligand (galanthamine) was performed. The resulting rmsd value of 0.1242 with the best-scored pose (−8.3437) demonstrated the algorithm's accuracy.

For the comparison of galanthine derivatives with other compounds, two additional *h*AChE enzymes crystallized with donepezil and a donepezil derivative were selected and retrieved from PDB.

The characterisation of these enzymes is following:

- **PBD ID:** 7E3H
- **PBD DOI:** 10.2210/pdb7E3H/pdb
- **Title:** Crystal Structure of Human Acetylcholinesterase in Complex with Donepezil
- **Organism:** *Homo sapiens*
- **Resolution:** 2.45 Å
- **R-Value Free:** 0.224
- **R-Value Work:** 0.194
- **Number of subunits** = 2 (100% homodimer, subunit A was selected)

- **PBD ID:** 7D9P
- **PBD DOI:** 10.2210/pdb7D9P/pdb
- **Title:** Crystal Structure of Recombinant Human Acetylcholinesterase in Complex with Compound 12
- **Organism:** *Homo sapiens*
- **Resolution:** 2.85 Å
- **R-Value Free:** 0.219
- **R-Value Work:** 0.180
- **Number of subunits** = 2 (100% homodimer, subunit A was selected)

Before docking, the enzymes were prepared in the same way as the first one, which involved removing subunit B, errors, and elimination of water molecules and excess ligands. Subsequently, protonation and restrained energy minimization were performed. The ligand was then defined in the prepared structure of the enzyme.

4.2.4.2 *In silico* preparation of ligands

For molecular docking, nine energy-minimized ligands were prepared using the MOE system, using the dominant protomer as predicted by MOE at pH 7.4. A 9-row database was then created. The structures of the isolated natural alkaloids (lycorine, galanthine, cherylline, **Figure 11**) were described in the literature and entered into the database using SMILES specifications, while the structures of the six semisynthetic derivatives of galanthine (synthesized and described in Master's thesis: LOJKÁSEK (2023)[67]) were created in ChemDraw (**Figure 12**).

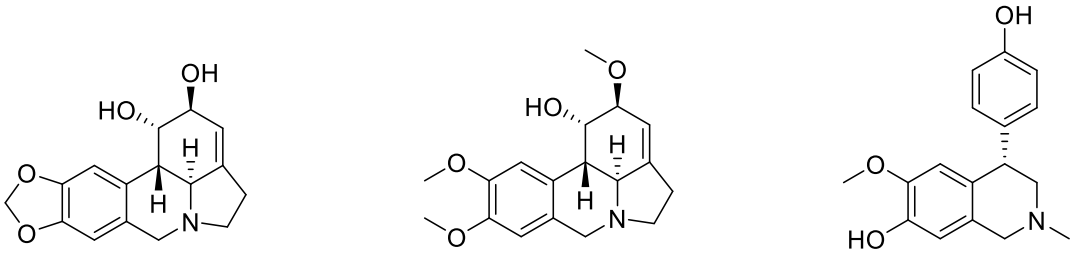

Figure 11. *Structures of isolated natural alkaloids 1–3.*

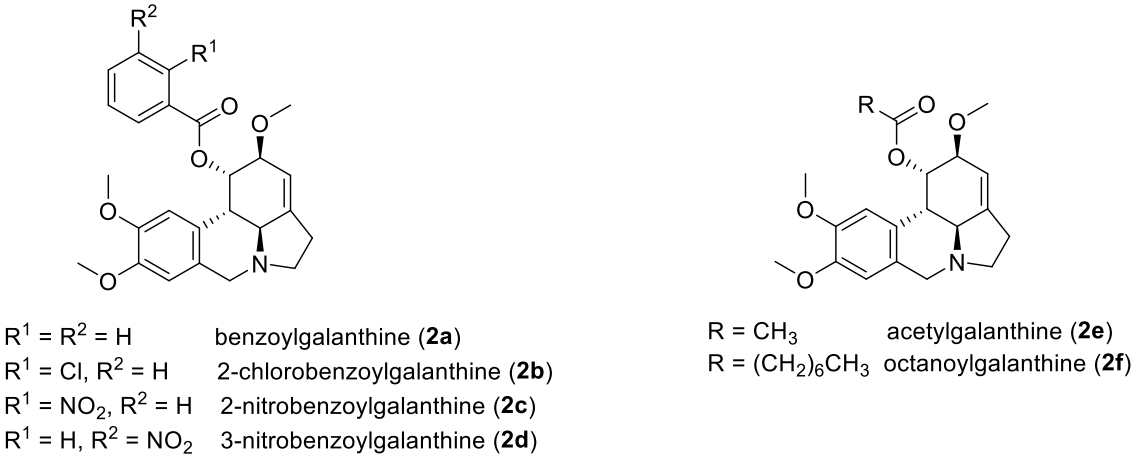

Figure 12. *Structures of semisynthetic derivatives of galanthine 2a–2f.*

The docking of flexible ligands was performed using a rigid receptor with default settings.

4.2.4.3 Determination of results

The main parameter for interpreting docking results is the Score (S) value, where the lowest value indicates the best position of the molecule. The data presented in the results were supplemented with the Ligand Efficiency (LE) value for completeness, which takes into account the differences between the size of the molecule and its affinity to the target site. LE was calculated according to the formula:

$$LE = \frac{Score}{N_{heavy}}$$

Where:

- **Score** is the binding affinity or binding free energy (ΔG) of the ligand.
- **N_{heavy}** is the number of heavy (non-hydrogen) atoms in the ligand.

4.3 Isolation of alkaloids

4.3.1 Preparation of alkaloid extract

Fresh bulbs (29 kg) were minced and completely extracted with EtOH (96%, v/v, 3×) by boiling for 30 min under reflux; the combined extract was filtered and evaporated to dryness under reduced pressure (**Figure 13** and **Figure 14**). The ethanolic extract (2.8 kg) was cleaned of ballast substances and non-alkaloid substances by liquid-liquid extraction (LLE).

Figure 13. *29 kg of fresh bulbs (left) and sliced bulb (right).*

Figure 14. *Bulbs processing. Mincing of bulbs with 96% EtOH (left) and heating a suspension under reflux (right).*

The crude extract was acidified to pH 1-2 with 2% HCl (5 L), and the volume of the suspension was made up to 7 L by water. The suspension was filtered. The filtrate was defatted by Et_2O

(3 × 2.8 L), alkalized to pH 9-10 with a 10% solution of Na_2CO_3, and extracted by EtOAc (3 × 2.5 L). The organic layer was evaporated to give 90 g of dark brown fluid residue. The aqueous phase was subsequently extracted also with $CHCl_3$ (3 × 1.5 L) to obtain alkaloids that were not soluble in EtOAc (**Figure 15**). The organic layer was evaporated to give 15 g of alkaloid extract. The aqueous phase was tested with Mayer's reagent for the presence of alkaloid.

Figure 15. *LLE after basification with EtOAc (left), and $CHCl_3$ (right).*

During the extraction with $CHCl_3$, 5.5 g of lycorine precipitated directly from the $CHCl_3$ solution. The lycorine was purified with $CHCl_3$ and EtOH and subsequently filtered over cotton.

The prepared extracts still contained a large amount of impurities, so the extraction was repeated once more. The entire process, starting from acidifying with HCl, was repeated for both extracts using 400 mL of 2% HCl, 5 × 250 mL of Et_2O, and 200 mL of 10% Na_2CO_3.

Finally, from the second LLE, 24.96 g of EtOAc alkaloid extract and 11.39 g of $CHCl_3$ alkaloid extract were obtained. The organic phase was dried using anhydrous Na_2SO_4, subsequently filtered through filter paper, and then evaporated using a rotavapor. The two alkaloid extracts were compared by analytical TLC (**Figure 16**) and GC/MS analysis, which detected that the occurrence of alkaloids was the same in both extracts. Based on this observation, it was decided to combine the fractions into one (36.35 g).

Figure 16. *Comparison of EtOAc and $CHCl_3$ extract.*

Preliminary HPLC/MS and GC/MS analyses were performed on this combined alkaloid extract to identify the alkaloids that could be expected in the extract.

4.3.2 Flash chromatography

The alkaloid extract was further fractionated by flash chromatography on silica gel. Before the separation process, the MP for flash chromatography was experimentally determined, ensuring the retention factor (Rf) was below 0.2. The MP of EtOAc:CH_2Cl_2 in a 75:25 ratio with Rf = 0.13 was chosen.

The pre-column for flash chromatography (120 g) was filled with the 36.4 g of alkaloid extract absorbed on 70 g of SiO_2 (1:2 ratio), and the remaining volume of the column was packed with SiO_2 (MERCK 40–63 µm).

The dimensions of the main column FC12 (12 x 250 mL) were 49 x 460 mm, with a dead volume of 600 mL. The column was packed in a suspension of 383 g of SiO_2 with CH_2Cl_2 under pressure, and air removal was achieved using the Flash system.

An initial washing was performed using a mixture of CH_2Cl_2 and EtOAc (starting at 25 % of EtOAc), followed by gradient elution up to 100 % EtOAc in 75 fractions (flow rate 60 mL/min and a maximum pressure of 16 bar). Fractions were collected in volumes of 90 mL (in peak) and up to 180 mL (between peaks), with tube changes performed at minima. Subsequently, MeOH was added to EtOAc, and another gradient elution was performed up to 100 % MeOH in 94 fractions. Finally, the column was washed with MeOH + acetic acid (99:1) at a flow rate of 100 mL/min and a maximum pressure of 16 bar. One acidic fraction was obtained from this cleaning, which was also stored.

Figure 17. *Flash chromatography, pre-column and column used for the extract separation.*

Flash chromatography yielded 168 fractions, which were compared using TLC and then combined into 18 fractions and one acidic fraction from cleaning of the column (**Table 5**, **Figure 18**). These fractions were subsequently evaporated and weighed. All fractions were analysed by HPLC/MS and GC/MS.

The acidic fraction was purified by LLE using 5% HCl and 300 mL of Et_2O. Alkaloids were extracted with 6 × 200 mL of $CHCl_3$ after basification with 125 mL of 10% Na_2CO_3.

Table 5. *Characterisation of flash chromatography fractions*

Fraction	Combined fractions	Weight [g]
1	1–9	0.13
2	10–13	0.12
3	14–33	0.44
4	34–42	0.12
5	43–45	0.31
6	46–53	0.95
7	54–69	1.75
8	70–87	2.95
9	88–114	2.30
10	115–123	1.40
11	124–129	1.82
12	130–132	1.21
13	133–142	5.11
14	143–147	1.89
15	148–152	3.03
16	153–160	3.36
17	161–164	0.94
18	165–168	0.31
19	Acidic fraction	0.27

The total weight of all fractions was 28.40 g.

***Figure 18**. Analytical TLC of final 18 + 1 fractions (MP: MeOH).*

In the tubes containing fractions 116 to 121 from flash chromatography, large crystals were observed (**Figure 19**). These crystals were further identified as **1** (700 mg).

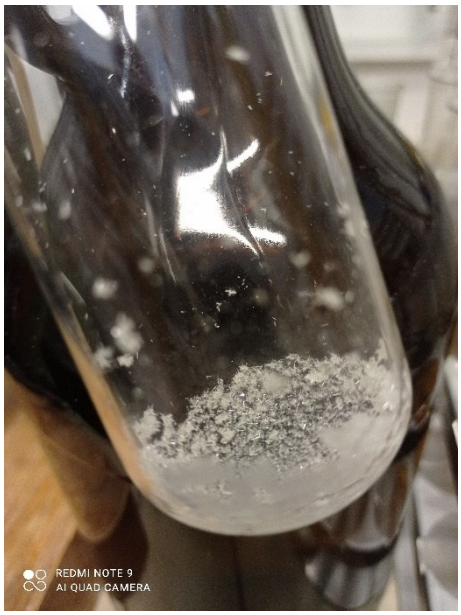

***Figure 19.** Crystals of **1** crystallized in the flash chromatography tube.*

4.3.3 Preparative TLC of fraction 8

For the purposes of this master's thesis, fraction 8, weighing 2.95 g, was chosen. Preparative TLC was preceded with GC/MS analysis to get a prediction of alkaloid occurrence. As shown in **Figure 20**, one major and one minor peak were observed in fraction 8.

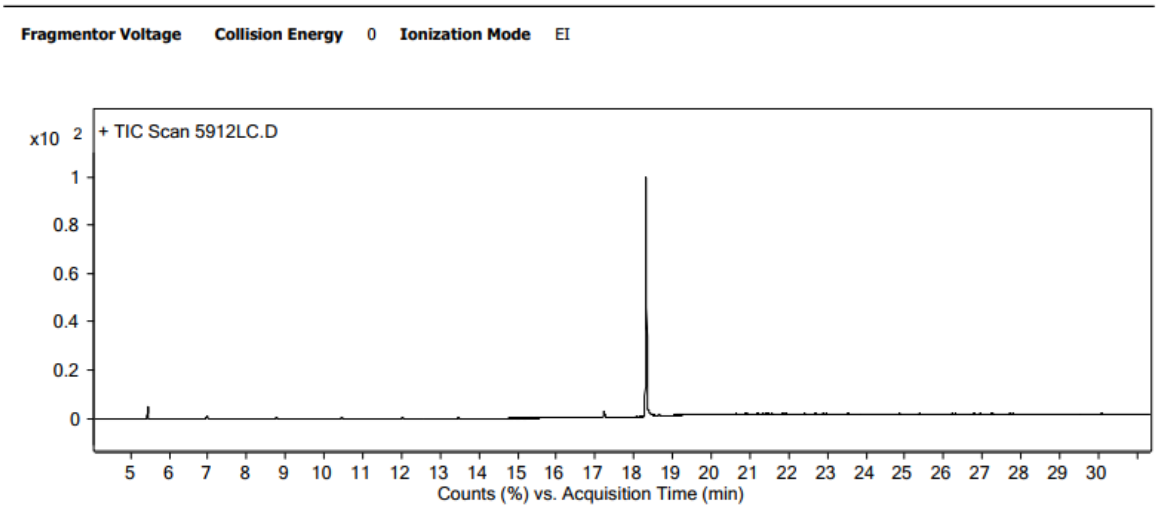

Figure 20. *GC/MS analysis of fraction 8.*

Using preparative TLC, fraction 8 was separated into 5 subfractions, using a MP of To:DEA (9:1) and 71 plates.

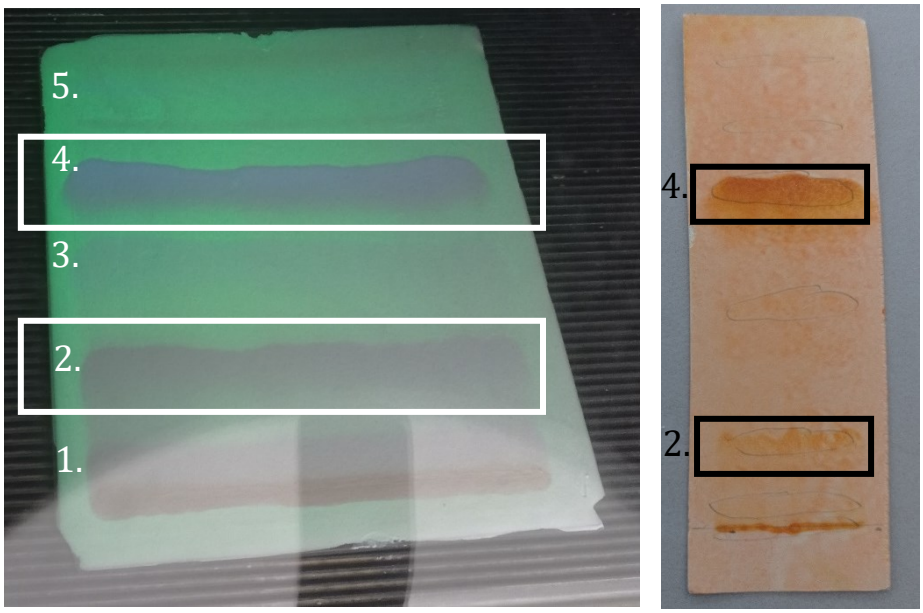

Figure 21. *TLC of fraction 8. Plate for preparative TLC under UV detection (left), and analysis TLC with Dragendorff's reagent detection (right) with highlighted zones for isolation of alkaloids (MP=To:DEA (9:1)).*

Table 6. *Weights of subfractions after initial separation*

Sub-fraction	**8-1**	**8-2**	**8-3**	**8-4**	**8-5**
Weight [mg]	339.4	209.3	120.3	1921.2	111.5

As observable from **Figure 21**, two zones contained significant amounts of alkaloids. It could be predicted that zone number 4 contained the major alkaloid (also significantly higher in weight), and zone number 2 contained the minor alkaloid. For a quantitative profile of separated subfractions see **Table 6**.

4.3.4 Isolation of alkaloids from 8-2 subfraction

Subfraction 8-2 was separated into other subfractions as described on **Figure 22** using MP and number of plates described in **Table 7**.

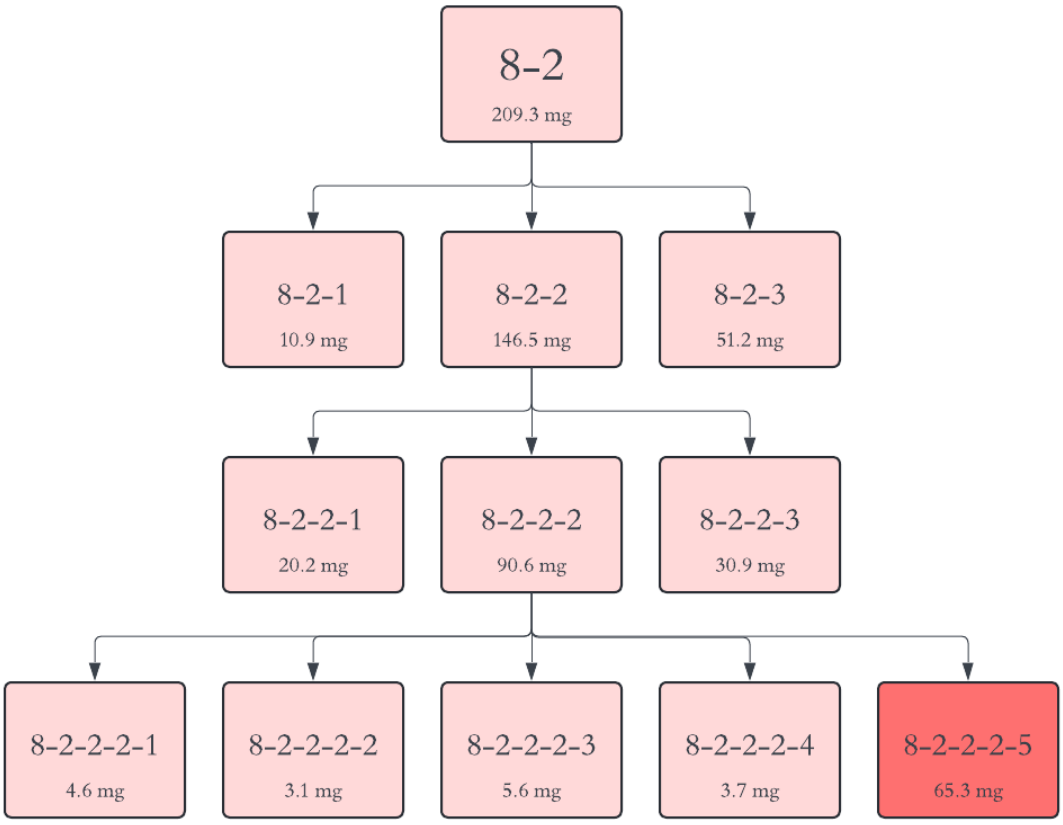

Figure 22*. Scheme of separation of subfraction 8-2 (with highlighted alkaloid-pure subfraction).*

Table 7. *Summary of MP and plates used during the separation of 8-2*

Subfraction	MP	Number of plates
8-2	To:MeOH (NH_4OH) 5:1 (0.1%) (3 × developed)	6 (pourable plates)
8-2-2	$CHCl_3$:MeOH (NH_4OH) 3:1 (0.1%)	3 (pourable plates)
8-2-2-2	$CHCl_3$:MeOH (NH_4OH) 3:1 (0.1%)	5 (commercial plates)

Figure 23*. Separation of subfraction 8-2-2. Alkaloid content detected by Dragendorff's reagent in subfraction 8-2-2-2 (MP= $CHCl_3$:MeOH (NH_4OH) (3:1(0.1%))).*

Subfraction 8-2-2 and further subfraction 8-2-2-2 were chosen due to alkaloid occurrence detected by Dragendorff's reagent, as observable in **Figure 23**.

Subfraction 8-2-2-2-5, which was alkaloid-pure, amounted to 65.31 mg and was subjected to GC/MS, HPLC/MS, NMR analysis, and optical rotation measurement.

During the separation, subfraction 8-2-2-2-2 also showed alkaloid activity, but this minor alkaloid was present in too low concentration for further analysis.

4.3.5 Isolation of alkaloids from 8-4 subfraction

As was previously mentioned, subfraction 8-4 showed the presence of the major alkaloid in fraction 8. For this reason, the subfraction was separated into additional subfractions as shown in **Figure 24**, with the MP and plates described in **Table 8**.

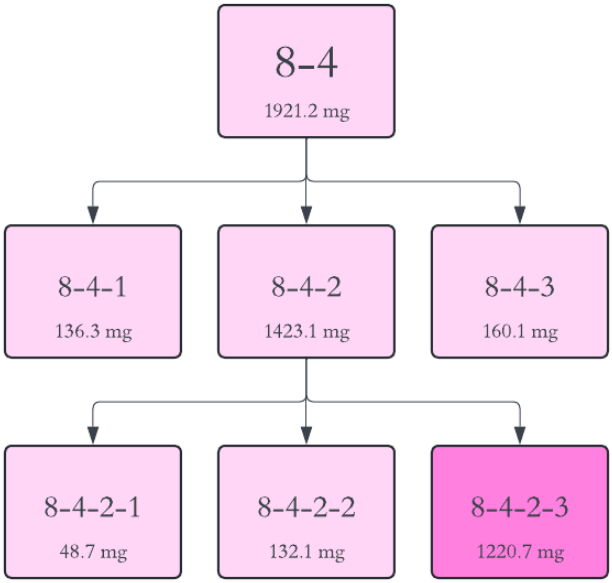

Figure 24. *Scheme of separation of subfraction 8-4 (with highlighted subfraction with major alkaloid content).*

Table 8. *Summary of MP and plates used during the separation of 8-4*

Subfraction	MP	Number of plates
8-4	ACN:EtOAc:MeOH:DEA 20:10:7.5:2.5	54 (pourable plates)
8-4-2	ACN:EtOAc:MeOH:DEA 20:10:7.5:2.5	41 (pourable plates)

Subfraction 8-4-2 was chosen, similarly to subfraction 8-2, due to the significant alkaloid presence detected by Dragendorff's reagent, as visible in **Figure 25**. As shown in this figure, alkaloid content was also visible in subfraction 8-4-1. Consequently, this subfraction was further separated, but the final concentration was again too low for further analysis.

Figure 25. *Separation of subfraction 8-4. Alkaloid content detected by Dragendorff's reagent in the subfraction 8-4-2 (MP=. ACN:EtOAc:MeOH:DEA (20:10:7.5:2.5)).*

However, subfraction 8-4-2-3 was not pure, therefore, it was purified by recrystallization from an ethanol-chloroform mixture. Finally, 1.2 g of pure crystalline substance was obtained and subjected to GC/MS, HPLC/MS, NMR analysis, and optical rotation measurement.

5 Results and Discussion

5.1 Structure evaluation

5.1.1 Alkaloid content prediction by GC/MS

Alkaloid content prediction was conducted before flash chromatography, and another prediction was performed for fractions after flash chromatography. For this analysis, GC/MS and HPLC/MS methods were used. The results of the GC/MS analysis were compared with the NIST library to predict the structure of the alkaloids. However, it is important to emphasize that these findings are primarily informative, as the similarity in chromatographic spectra between compounds does not allow for definitive confirmation of their exact content.

First, the prediction of alkaloid content was performed for EtOAc and $CHCl_3$ alkaloid extracts. The GC/MS analysis of the EtOAc extract revealed a broader range of alkaloids compared to the $CHCl_3$ extract. But since the major alkaloids (lycorine, galanthine, pancracine) were presented in both extracts, they were combined, as mentioned in section **4.3.1** and further separated on flash chromatography. GC/MS analysis was then performed on the 19 obtained fractions, which is summarized in **Table 9**.

The corresponding MWs were also detected in HPLC/MS analysis as protonated molecules. Analysis by both GC/MS and HPLC/MS is necessary because GC/MS may not detect non-volatile compounds.[68]

***Table 9**. Alkaloids identified in fractions from flash chromatography separation*

Fraction	Compound	RT (min)	$[M^+]$ and characteristic ions, m/z (% relative intensity)	Probability (%)	Data file at the department	Matching MW from HPLC/MS
1		Column impurities			5905LC.D	-
2		Column impurities			5906LC.D	-
3		Matches under 85%			5907LC.D	-
4		Matches under 85%			5908LC.D	-
5		Matches under 85%			5909LC.D	-
6		Matches under 85%			5910LC.D	-
7	cherylline	17.242	285(39), 242(100), 241(94), 225(84), 211(65), 181(31)	98.4	5911LC.D	285

Fraction	Compound	RT (min)	[M^+] and characteristic ions, m/z (% relative intensity)	Probability (%)	Data file at the department	Matching MW from HPLC/MS
7	galanthine	18.311	317(17), 268(16), 243(86), 242(100), 162(10), 125(9)	96.5		317
8	cherylline (minor)	17.231	285(31), 242(100), 241(85), 225(88), 211(70), 181(31)	95.6	5912LC.D	285
	galanthine (major)	18.314	317(18), 268(14), 243(87), 242(100), 162(10), 125(11)	96.8		317
9	galanthine (major)	18.306	317(15), 268(17), 243(87), 242(100), 162(12), 125(14)	95.8	5913LC.D	317
10	lycorine (major)	18.631	287(21), 250(27), 227(57), 226(100), 147(11)	91.2	5914LC.D	287
11	lycorine (major)	18.629	287(19), 250(26), 227(61), 226(100), 147(11)	90.5	5915LC.D	287
12	3-acetylpancracine	18.444	329(91), 281(40), 270(56), 268(72), 223(74), 207(100), 185(62)	84.8	5916LC.D	-
	lycorine	18.626	287(21), 250(23), 227(61), 226(100), 147(11)	90.2		287
13	3-acetylpancracine	18.441	329(100), 281(30), 270(62), 268(80), 223(91), 207(96), 185(57)	91.0	5917LC.D	-
14	lycorine (major)	18.640	287(22), 250(23), 227(61), 226(100), 147(11)	92.8	5918LC.D	287

Fraction	Compound	RT (min)	[M^+] and characteristic ions, m/z (% relative intensity)	Probability (%)	Data file at the department	Matching MW from HPLC/MS
14	narcissidine	19.819	332(22), 315(52), 284(100), 266(38), 258(51), 230(63), 228(55), 207(35)	96.8		333
15	pancracine (major)	18.159	287(100), 243(26), 223(29), 199(37), 185(42)	89.3	5919LC.D	287
	lycorine	18.620	287(22), 250(20), 227(62), 226(100), 147(12)	85.5		287
	narcissidine	19.830	332(20), 315(48), 284(100), 266(37), 258(45), 230(55), 228(47), 207(21)	96.4		333
16	pancracine (major)	18.159	287(100), 243(23), 223(27), 199(33), 185(41)	87.8	5920LC.D	287
	narcissidine	19.816	332(28), 315(53), 284(100), 266(40), 258(54), 230(68), 228(57), 207(90)	93.8		333
17	pancracine (major)	18.156	287(100), 243(23), 223(30), 199(32), 185(39)	89.4	5921LC.D	287
18		Matches under 85%			5922LC.D	-
Acidic		Matches under 85%			5923LC.D	-

Comparing the composition of alkaloid content with the study on *N. poeticus* var. *recurvus* by Cahlíková and co-workers,[7] four alkaloids out of six reported were detected as well, namely lycorine, pancracine, galanthine, and cherylline. Ločárek and co-workers additionally reported 3-acetylpancracine,[14] which was also detected in our analysis. As these studies described only a GC/MS analysis of the whole extract, the fractions obtained after the separation revealed one more alkaloid — narcissidine. However, the real presence of these alkaloids could only be confirmed

by through structure elucidation of pure compounds (NMR analysis, X-ray crystallography, chiroptical methods) or a combination of MS analysis against the corresponding standard sample.

Fraction 7 was already described in the master's thesis of Lojkásek,[67] where the prediction of alkaloids **2** and **3** (mentioned in **Table 9**) was confirmed. Other fractions are still in the process of isolation and will be described in future master's theses or a summary article.

5.1.2 Structure evaluation of isolated alkaloids

Three alkaloids were finally isolated for the purposes of this master's thesis. All of them are known alkaloids, already described in the literature.

5.1.2.1 Lycorine

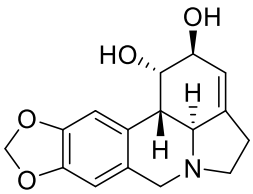

Chemical Formula: $C_{16}H_{17}NO_4$
Molecular Weight: 287,32

Figure 26. *Structure of **1**.*

Compound **1** was isolated by crystallisation after flash chromatography (**Figure 19**) and during LLE (**4.3.1**). This alkaloid was isolated at a weight of 6.2 g.

The prediction from GC/MS analysis (**Table 9**) was confirmed by MS, optical rotation and NMR spectroscopy, with the following results:

- MW = 287
- $[\alpha]_D^{25}$= −64 (c = 0.05 g/100 mL, $CHCl_3$ + EtOH)
- NMR data were in agreement with published data[47]
- GC/MS *m/z*: 287(21), 250(27), 227(57), 226(100), 147(11).

Considering the physical properties of **1**, it is completely insoluble in petroleum ether, Et_2O, and $CHCl_3$ but displays moderate solubility in EtOAc, Ac, and MeOH.[46] This poor solubility of **1** is an important point for discussion due to its significant anticancer activity described below. Low solubility hinders the effective preparation of pharmaceutical forms for the application of this compound. That is why scientists are trying to improve lycorine's water dispersibility and prolong its half-life.[69]

Using DMSO as a solvent for the preparation of NMR samples, instability was observed. This instability occurred after a few hours and manifested as a colour change from colourless to yellowish. However, it is important to mention that many compounds are unstable when stored

at room temperature, even in a DMSO solution. The study on the stability of chemical compounds in DMSO indicates that approximately 18% of the compounds underwent degradation after being stored at room temperature for a period of five months.[70]

As was already mentioned (in section **4.2.3.3**) impurity was observed in the lycorine sample. However, not many descriptions of **1** degradation could be found in the literature. In an old study by Cook and co-workers,[71] a summary of previous studies about degradation products of **1** is provided, most of which were synthesized. Also with the poor solubility profile of **1**, there is a question of impurity due to degradation or incomplete purification during isolation. The impurity structure was not identified due to its low concentration. For further study, there is an idea to apply this purification process on a larger scale of the impure sample of **1** to structure and evaluate the impurity.

It is worth noting that the degradation of natural products due to environmental conditions or during the isolation process is a significant concern in phytochemistry. One of the main problems during the manipulation is chemical instability (dehydration, rearrangement, and oxidation reactions) and thermal factors.[72] Another problem that can occur during the isolation process is the appearance of solvent-derived artefacts in natural products. Alcoholic solvents can give the source of ethoxy- or methoxy-derivatives. While ethoxy groups are very rare in nature, it is not easy to determine if methoxy compounds are natural or byproducts of contamination.[73]

5.1.2.2 Galanthine

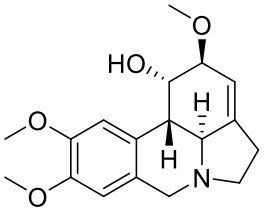

Chemical Formula: $C_{18}H_{23}NO_4$
Molecular Weight: 317,39

Figure 27**. Structure of **2.

The major alkaloid of fraction 8, compound **2**, was isolated from subfraction 8-4, as described in section **4.3.5.** The white crystals shown in **Figure 28** (total 1.2 g) were obtained after recrystallization or crystallization in vacuo using a rotary evaporator.

***Figure 28**. Crystals of **2** after evaporation of solvent under the vacuum.*

The prediction of this major alkaloid was confirmed by MS, optical rotation, and NMR spectroscopy, with the following results:

- MW = 317
- $[\alpha]_D^{25}$= −32 (0.10 g/100 mL, $CHCl_3$)
- NMR data were in agreement with published data[74]
- GC/MS *m/z*: 317(17), 268(16), 243(86), 242(100), 162(10), 125(9).

5.1.2.3 Cherylline

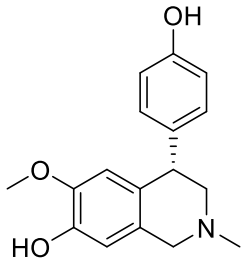

Chemical Formula: $C_{17}H_{19}NO_3$
Molecular Weight: 285,34

Figure 29. *Structure of* ***3****.*

The minor alkaloid of fraction 8, compound **3**, was obtained from subfraction 8-2 (**4.3.4**) as 65.31 mg of yellow or yellow-brown crystals, as shown in **Figure 30**.

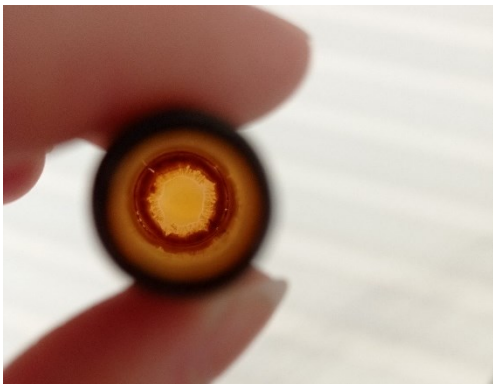

Figure 30. *Crystals of* ***3*** *at the bottom of the vial.*

The prediction of this minor alkaloid was confirmed by MS, optical rotation and NMR spectroscopy, with the following results:

- MW = 285
- $[\alpha]_D^{25} = +16$ (0.05 g/100 mL, $CHCl_3$ + EtOH)
- NMR data were in agreement with published data[75]
- GC/MS *m/z*: 285(39), 242(100), 241(94), 225(84), 211(65), 181(31).

5.2 *In vitro* analysis

Another main aim of this study was to determine the biological activity of isolated compounds, focusing primarily on their potential anticancer activity and their implications for AD treatment.

For this purpose, three different biological tests were conducted on the isolated compounds.

5.2.1 Inhibitory activity against *h*AChE and *h*BuChE

The results determined by Ellman's spectrophotometry method are shown in **Table 10**.

Table 10. *Inhibitory activity of alkaloids against hAChE and hBuChE*

compound	**structural type**	***h*AChE IC_{50} [µM]**	***h*BuChE IC_{50} [µM]**
lycorine **(1)**	lycorine	>100	>100
galanthine **(2)**	lycorine	>100	>100
cherylline **(3)**	cherylline	>100	11.34 ± 0.88
galanthamine HBr*	galanthamine	2.01 ± 0.14	33.69 ± 2.66
eserine*	indole	0.20 ± 0.01	0.30 ± 0.01

* reference compounds

From the results, it was evident that our alkaloids exhibit no inhibitory activity against *h*AChE. These findings have already been published in many studies for **1** by Cao and co-workers,[76] and also by Ka and co-workers, who described weak activity for **3**.[77] Hulcová and co-workers reported no inhibitory activity for both *h*AChE and *h*BuChE for **2**.[78] The literature provided an interesting comparison with AChE from a different source, the electric eel, where the IC_{50} value for **2** was 1.96 ± 0.01 µM. However, these results cannot be directly compared due to different sources of the enzyme.[79] No inhibitory activity was also reported for *h*BuChE and lycorine.[80]

Compound **3** demonstrated good inhibitory activity against *h*BuChE, a finding that has not been previously reported. This result is promising for further research, as highlighted by Wang and colleagues, who noted that selective BuChE or bivalent ChE inhibitors could represent a novel approach to treating AD.[81] Moreover, this study successfully identifies **3** as the specific compound responsible for the *h*BuChE inhibitory potential (IC_{50} = 23.0 ± 1.0 µM) initially reported by Cahlíková and co-workers.[7] Notably, this inhibitory activity is higher than that observed for **3**,

indicating that there may be other compounds in the plant with lower inhibitory activity against *h*BuChE than **3**.

5.2.2 Cytotoxicity screening

Cytotoxicity screening was determined on the cell lines mentioned in section **4.1.2.2. Table 11** describes the cytotoxicity screening of **3**.

Table 11. *Cytotoxicity screening of cherylline in GP*

cell line	DMSO	3	doxorubicin
Jurkat	100	96	6
MOLT-4	100	99	3
A549	100	105	11
HT-29	100	105	46
PANC-1	100	86	56
A2780	100	103	47
SHSY5Y	100	105	5
MCF-7	100	96	21
SAOS-2	100	103	14
MRC-5	100	114	54

Comparing **3** with doxorubicin (positive control), **3** is significant without anticancer activity. This cytotoxicity screening presents new data for **3** that have not been published before and made from **3** potential candidate for the AD research field, thanks to good *h*BuChE inhibitory activity.

Regarding the data in the literature, the only report by Ka and co-workers specified a biological test for the MCF-7 cell line with interesting results.[77] In this study, anticancer activity for MCF-7 is described but only at higher concentrations of cherylline (400 µM), where GP is approximately 17%, a value comparable to lycorine activity.[77] Another study by Antonio Evidente described weak cytotoxicity at 100 µM concentration.[82] This observation suggests that further tests of cherylline at higher concentrations could be valuable. The key question is whether this alkaloid remains non-cytotoxic to healthy cells at these higher concentrations.

For the two other alkaloids, **1** and **2**, cytotoxicity screening was also determined by Havelek and co-workers, and the results were already published.[83] The results for the same cell lines as for cherylline, except SHSY5Y, are shown in **Table 12**, with the non-tumour cell line - Normal human dermal fibroblasts (NHDF).

Table 12. *Cytotoxicity screening of **1** and **2** in GP by Havelek and co-workers*[83]

cell line	DMSO	1	2	doxorubicin
Jurkat	113	5		4
MOLT-4	115	9	103	2
A549	106	27	93	46
HT-29	87	5	64	16
PANC-1	95	36	97	63
A2780	98	39	163	45
MCF-7	99	27	114	52
SAOS-2	102	27	97	23
NHDF	93	34	112	48

These results show that **1** is an active anticancer compound, as already described in many studies for a broad range of cell lines.[84] In contrast, **2** is completely devoid of cytotoxic activity, as evidenced not only by this study but also by two other studies by Katoch and co-workers[48] and by Van Goietsenoven and co-workers.[85]

Another cytotoxicity screening for the MCF-7 cell line using the MTS method, described in section **4.2.3.3** brought different results, as shown in **Table 13**.

Table 13*. IC_{50} determination in breast cancer cell line MCF-7*

compound	IC_{50} MCF-7 [µM]
1	>50
2	>50
3	1.41

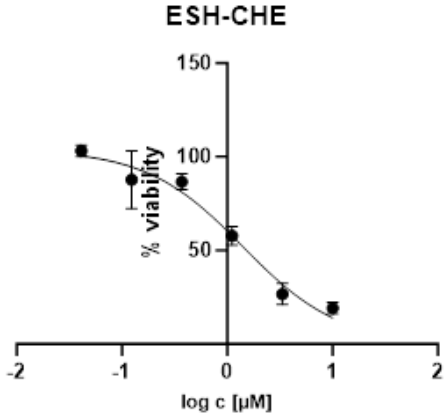

Figure 31. *A dose-response curve of **3**.*

By comparing the results, diametrically different outcomes were observed. **Table 13** shows compound **3** as a compound with good anticancer activity against the MCF-7 cell line, which is contrary to **Table 11**. As determined in **Figure 31**, the viability of cells decreased with the increasing concentration of **3**. This observation is consistent with the study by Ka and co-workers,[77] described above. However, in this assay, the same concentration of the compound was used as in the previous one, but with a different incubation time. The first assay used 48 hours, while the second used 72 hours regiment. Longer exposure to the compound can increase its cytotoxicity on cells, as described in the study.[86]

However, considering the result for **1** (**Table 13**), this does not correspond with the broad range of studies[46,81,87,88] describing its good anticancer activity against the MCF-7 cell line (**Table 12**). For this reason, it is suggested to repeat the determination of anticancer activity against the MCF-7 cell line for more certain results.

5.2.3 Inhibition of topoisomerase IIα

Anticancer activity through the mechanism of action by inhibition of Topo IIα was determined for three isolated alkaloids.

Table 14. *Inhibitory activity of alkaloids against Topo IIα*

compound	IC_{50} Topo IIα [μM]
1	>100
2	>100
3	>100
QAP-1 (standard)*	0.73 ± 0.03

**N*^{6}-(*tert*-butyl)-8-ethyl-*N*^{2}-(2-(2-morpholinoethoxy)quinolin-6-yl)-7*H*-purine-2,6-diamine, known, potent ATP-competitive inhibitor of Topo IIα from *Novartis*

Niño and co-workers described good inhibitory activity of **1** against human Topo I.[89] There was a question of whether **1** could also inhibit Topo IIα. The assay was also applied to **2** because it is of the same (lycorine) structure type and to **3** because no study had tested it before. However, as the results in **Table 14** show, there is no promising inhibitory activity. Therefore, it might be interesting for further study to test **2** for Topo I inhibition.

5.2.4 Additional activity testing

Beyond the primary aim of this master's thesis, other activities were also evaluated. The antifungal and antibacterial activities for **1** and **2** were previously published by our department in a study by Ločárek and co-workers[14], which reported no significant inhibitory activity. Compound **3** had not been tested before at our department, and similarly, our test showed no significant inhibition.

5.3 *In silico* analysis

Molecular docking is a useful tool for predicting interactions with drug targets, which can guide synthesis decisions in the preparation of derivatives.[90] Additionally, retrospective analysis of synthesized derivatives can provide insights into interaction potential and assist in structural modifications.

To interpret the docking results, it is important first to understand the binding interactions of the crystallographic galanthamine (**4**) within the enzyme.

Describing **Figure 32** the active site of the enzyme is the ester site, consisting of three amino acids (catalytic triad): His(447), Glu(202), and Ser(203). In this area, the interaction of Glu with the free OH group can be observed, where we assume a hydrogen bond. Another significant component is the anionic site, where Trp(86) plays an important role, leading to significant H-Ar interactions. Additional Ar-H bonds can also be observed with Gly(121) and Phe(297) (which are part of the oxyanionic site and acyl site). These interactions can be considered stabilizing within the binding site. The final interaction is an ion-dipole interaction between Asp(74) and the protonated tertiary nitrogen, which can also be considered significant for stabilizing the binding within the active site. This description is confirmed by Dvir and co-workers[91] as shown in **Figure 33**.

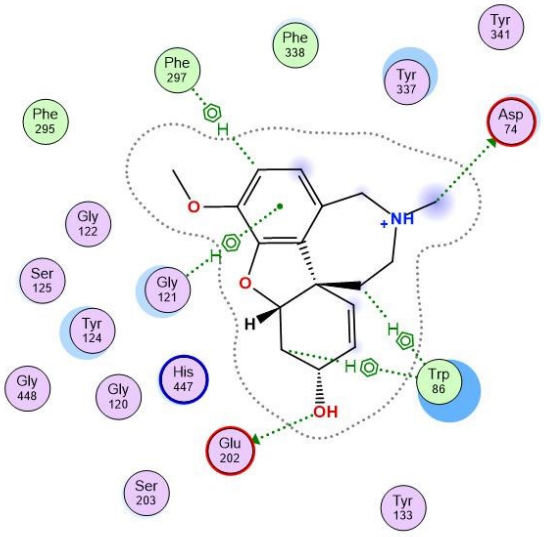

Figure 32. *Description of binding interactions of* ***4*** *in the hAChE enzyme.*

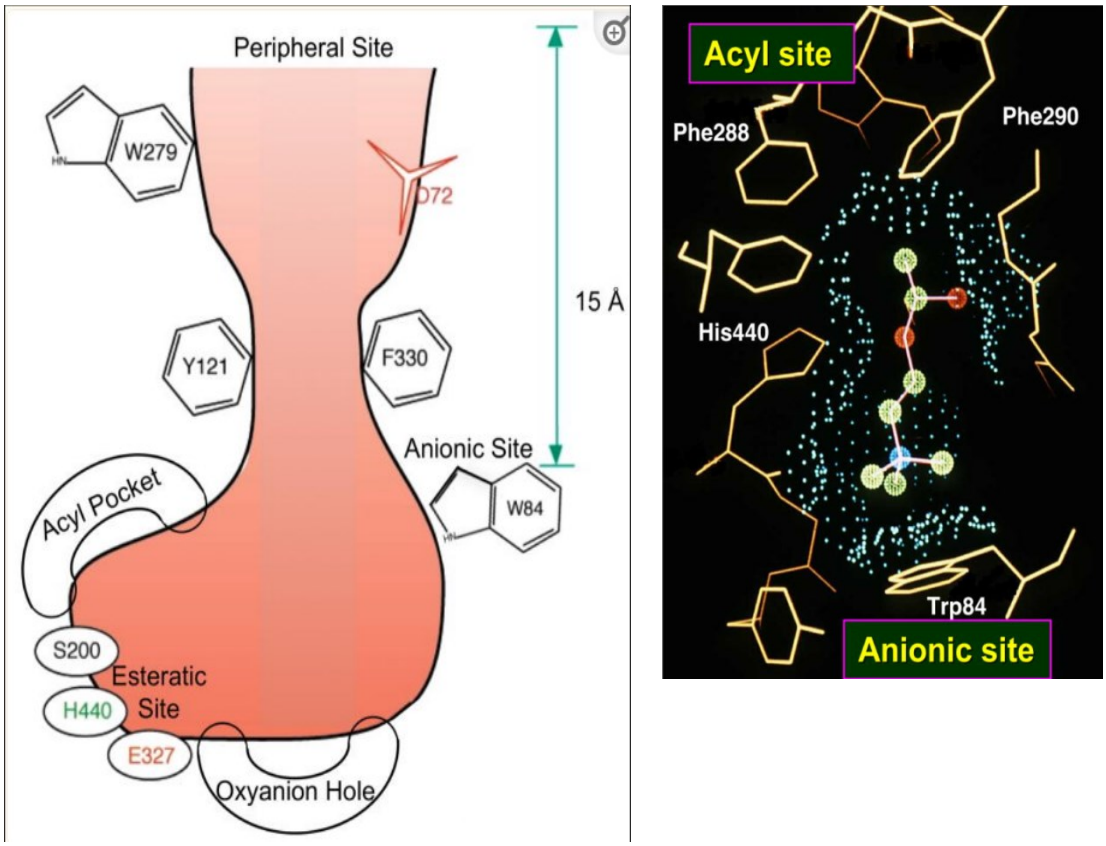

Figure 33. *Graphic representation of AChE by Dvir and co-workers.*[91]

Unless otherwise stated, molecular docking was performed into the enzyme with PBD ID: 4EY6.

5.3.1 Comparison of docked positions of parent alkaloids with crystallographic ligand

3D overlays describe different types of interactions of three parent alkaloids compared to the crystallographic ligand, aiming to define which interactions are crucial for inhibitory activity.

1. **Superposition of crystallographic galanthamine (4) with lycorine (1)**

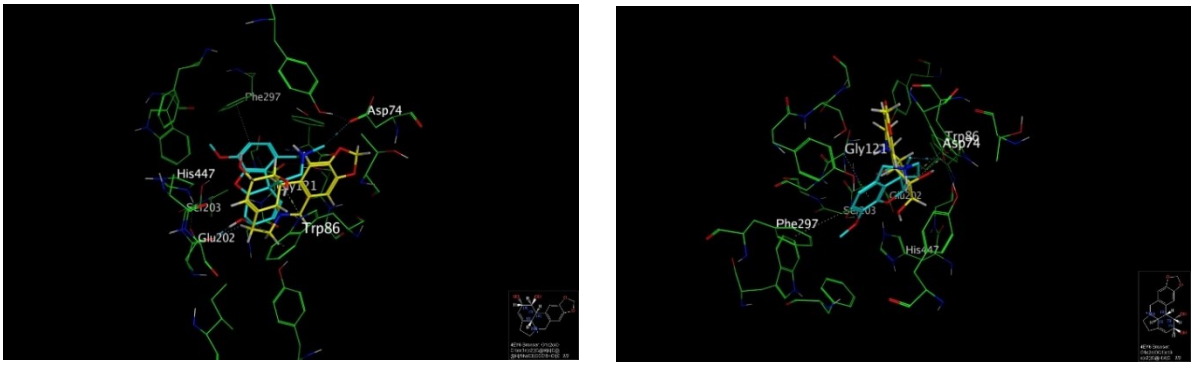

Figure 34. *4 (blue) vs 1 (yellow) underlining different interactions in the active site (left), and different orientations in the cavity (S = -6.53400) (right).*

Figure 34 shows a common interaction of **4** and **1** with Glu(202) in the catalytic triad. This hydrogen bond interaction is described as the main one for **4.**[92] However, the active site interaction does not necessarily guarantee inhibitory activity. Comparing the biological activities of these alkaloids shows a significant difference, the IC_{50} (*h*AChE) for **4** is 1.07 µM, while for **1** it is >100 µM. This disparity can be attributed to different orientations in the cavity, particularly regarding the nitrogen location, which, as seen in a 3D overlay of the lowest score, is in the opposite direction compared to **4**. **Figure 34** further highlights the different positions of **1**. The lack of good inhibitory activity may also be due to the absence of stabilizing bonds (hydrophobic interactions, ion-dipole interaction with nitrogen).

Description of the binding mode of 1

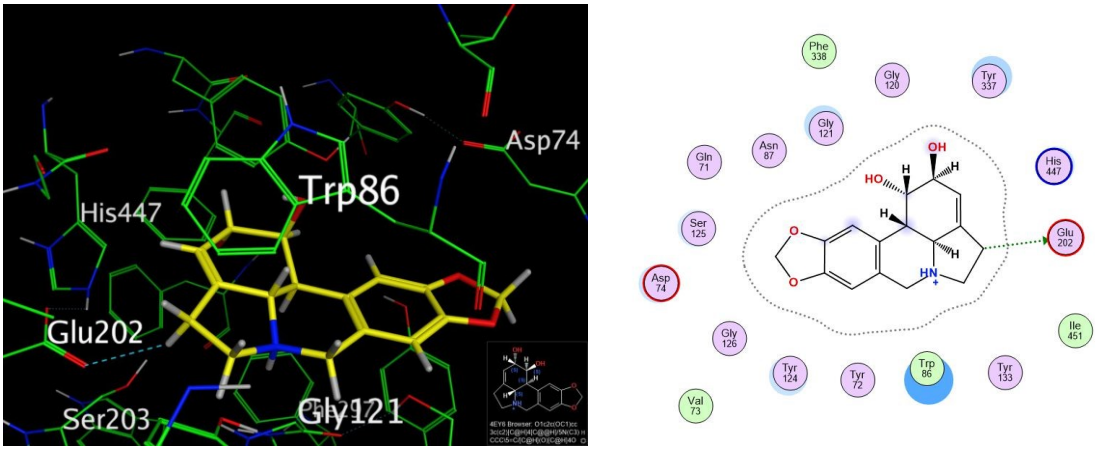

Figure 35*. 3D interaction scheme (left) and 2D interaction scheme of 1 (right).*

In the 2D interaction scheme (**Figure 35**), we observe a hydrogen bond with Glu(202), the active site of the enzyme. The change in position did not result in any significant alterations in the interactions.

2. Superposition of crystallographic galanthamine (4) with galanthine (2)

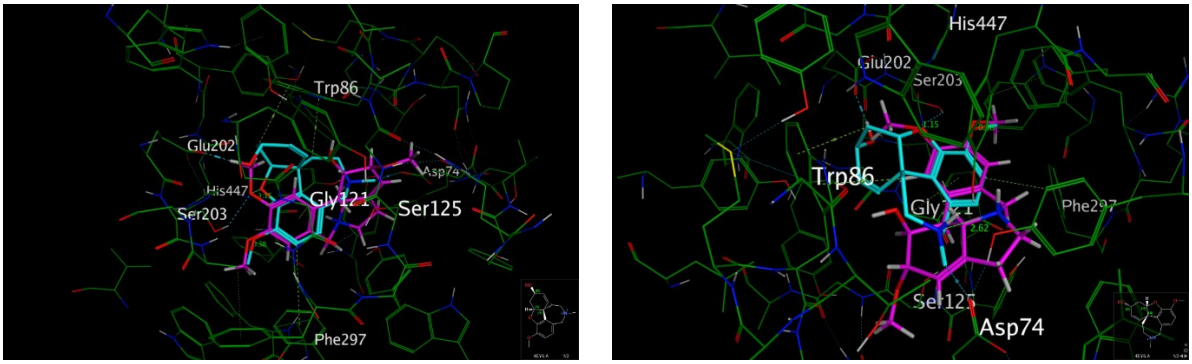

***Figure 36. 4** vs **2**, S = –6.421 (left), and overlay signalizing pharmacophore match (right).*

The best position of **2** in the cavity was observed at S = –6.421, demonstrating interaction in the active site of the enzyme (**Figure 36**). In comparison, **4** interacts with Glu(202), while **2** interacts with Ser(203). According to literature, another study describes a hydrogen bond between an oxygen of **4** and a hydrogen of the Ser(203) hydroxyl group.[93] Nonetheless, examining the pharmacophore characteristics, good matches of methoxy groups, aromatic rings, and ether oxygen are observable in superposed ligands. Considering nitrogen interaction as a potentially crucial interaction, it is clear that the discussed pose is the best one due to the close positioning of nitrogen in superposed ligands.

Description of the binding mode of 2

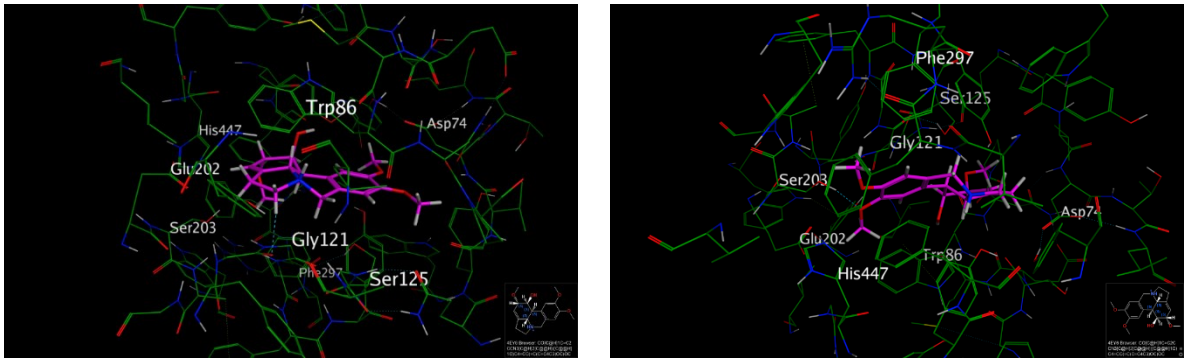

***Figure 37.** 3D interaction scheme of 2, for S = −7.291 (left), and for S = −6.421 (right).*

Notably, no interaction was observable in the pose with the lowest score of **2**. However, at S = –7.291, a hydrogen bond with Gly(121) is presented, and at S = –6.421, an interaction in the active site of the enzyme with Ser(203) is noted (**Figure 37**). This interaction is particularly significant because, in comparison with *Tc* (*Torpedo californica*) AChE described in the literature, there was no interaction with Ser(200).[79] Induced-fit docking was performed for **2**, but unfortunately, it did not bring any new results.

3. Superposition of crystallographic galanthamine (4) with cherylline (3)

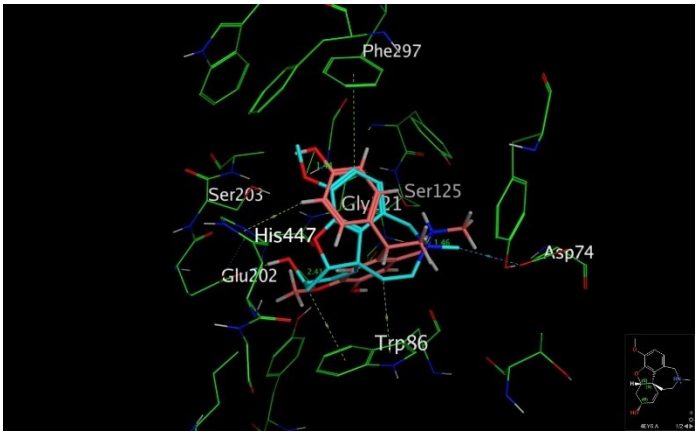

***Figure 38**. **4** vs **3**, S = –7.256.*

At the lowest score (–7.256), interesting matches with **4** are observable (**Figure 38**), even though **3** has a different structural type. Notably, a significant interaction with His(447) from the catalytic triad is observed. The pharmacophore properties are also noteworthy, in the superposed ligands, the layouts of aromatic rings and the proximity of the oxygens in methoxy and hydroxy groups are evident. While crucial interactions in the active site and structure orientation are observable, the inhibitory activity for *h*AChE is >100 µM, meaning that no activity was detected. However, a good activity (IC_{50} = 11.34 µM) for *h*BuChE has been demonstrated, indicating high selectivity of the compound.

Description of the binding mode of 3

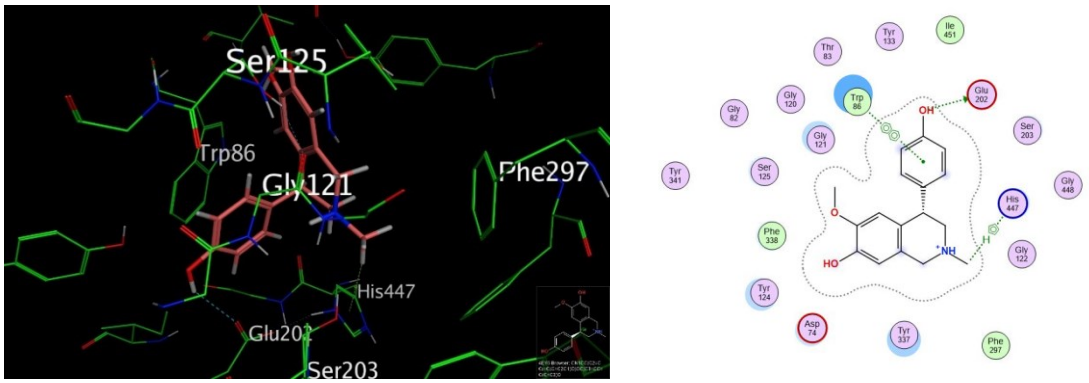

***Figure 39.** The best interaction potential of **3**, S = –6.513 (left); and 2D interaction scheme of **3**.*

At S = –6.513 (**Figure 39**), the best interaction potential of a molecule is demonstrated by interactions with His(447) and Glu(202) in the active site of the enzyme. Meanwhile, at S = –6.855, there is an interaction with Asp(74), and at S = –7.256, there is another interaction with His(447).

Table 15. *Comparison of interaction potentials of parent alkaloids*

Alkaloid	Score	Hydrogen bond residue	Aromatic interactions residue	Ion-dipole interaction residue	LE	Number of heavy atoms	*h*AChE IC_{50} [μM]
1	−6.5340	Glu(202)			−0.3111	21	>1000
	−6.5055	Glu(202)			−0.3098	21	
2	−7.2910	Gly(121)			−0.3170	23	606.92 ± 60.45
	−7.1120	Ser(203)			−0.3092	23	
	−6.9930	Ser(203)			−0.3040	23	
	−6.4210	Ser(203)			−0.2792	23	
3	−7.2563		His(447)		−0.3455	21	>100
	−6.8551	Asp(74)			−0.3264	21	
	−6.5128	Glu(202)	His(447), Trp(86)		−0.3101	21	
4	−8.3437	Glu(202)	Gly(121), Phe(297), Trp(86)	Asp(74)	−0.3973	21	1.710 ± 0.065

As indicated in **Table 15**, none of the parent alkaloids exhibit as broad a range of interactions as **4**, particularly in terms of stabilization through aromatic and ion-dipole interactions. This could be a critical factor in the lower inhibitory activity of these parent alkaloids compared to **4**. Although **3** shows a broader interaction scale, it is not an effective inhibitor of *h*AChE. The lack of significant *in vitro* activity compared to *in silico* predictions can be attributed to various factors, including solubility, membrane permeability, and plasma protein binding.[94] However, **3** is a selective inhibitor of *h*BuChE (IC_{50} = 11.34 μM). Molecular docking to *h*BuChE is planned for further study of **3** to compare its interaction potential with *h*AChE inhibition.

Despite the low inhibitory activity of parent alkaloids, their good isolation profile allows for the easy synthesis of semisynthetic derivatives. Numerous studies have produced galanthamine derivatives with nanomolar IC_{50} activities.[24] Notably, one galanthamine derivative in the study by Stavrakov and co-workers exhibited an IC_{50} of 27.79 nM, making it 68 times more active than galanthamine.[95] Galanthamine derivatives provide a good example of the application of molecular docking in drug design, as demonstrated by the docking-based model for predicting newly designed galanthamine derivatives by Atanasova and co-workers.[96] This is why a molecular analysis of galanthine derivatives was conducted.

5.3.2 Docking results of derivatives of galanthine

As mentioned in **Figure 12**, six different semisynthetic derivatives of **2** were tested by molecular docking. Analyzing the orientation of the molecules in the *h*AChE cavity and their binding interactions, the best results were observed for derivatives 2-chloro (**2b**) and 3-nitro (**2d**).

Table 16. *Docking and biological characteristics of galanthine derivatives*

Derivative	Lowest Score	Best LE	*h*AChE[1] IC_{50} [μM]	AChE (% inhibition) at 10 μM
2a	−7.4517	−0.2921	>10.00	20.94 ± 2.11
2b	−7.3788	−0.2062	>10.00	7.45 ± 1.50
2c	−7.2358	−0.2007	*	*
2d	−8.5732	−0.1926	>10.00	29.59 ± 2.09
2e	−8.5165	−0.3069	>10.00	23.29 ± 0.48
2f	−8.5734	−0.2210	>10.00	4.28 ± 0.89

***2c** was prepared in low yield to measure biological activity

Table 16 clearly shows that the lowest score or higher LE does not guarantee good binding interactions and orientation in the cavity. For this reason, it is necessary to analyse molecules with similar orientations in the cavity (**Figure 40**) as the parent alkaloid **2** individually, rather than relying only on statistical data from the database.

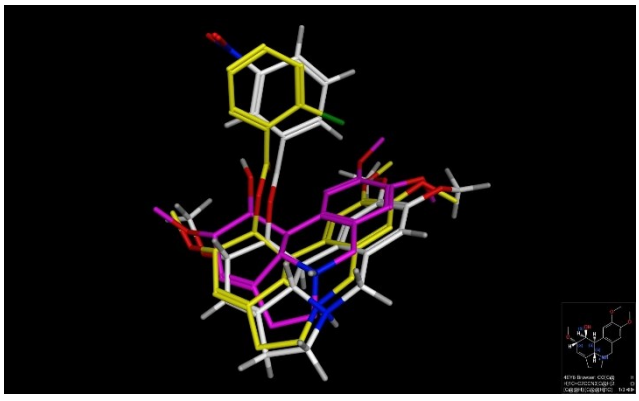

Figure 40. *Overlay of parent alkaloid **2** (magenta) with derivative **2b** (yellow) and **2d** (white).*

[1] Biological activities of semisynthetic derivatives were measured in Master's thesis: LOJKÁSEK (2023)[67]

In **Figure 40**, a perfect overlay of the parent alkaloid **2** and its semisynthetic derivatives is shown. In contrast, **Figure 41** shows a different orientation of **2a**, which is due to the absence of substituents on the benzene ring. From this observation, we can conclude that the substitution of the benzyl group in the derivatives is a crucial factor for fitting to the enzyme's cavity.

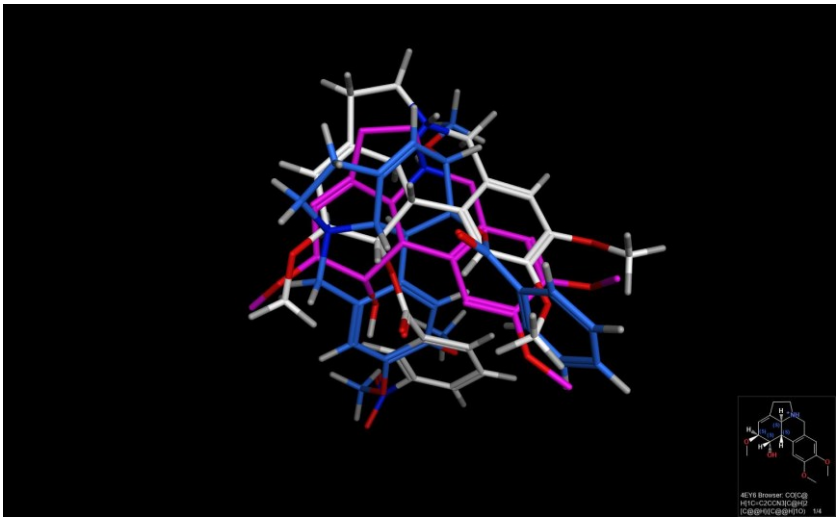

Figure 41. *Overlay of parent alkaloid* ***2*** *(magenta) with* ***2d*** *(white) and* ***2a*** *(blue).*

Orientation in the cavity

The shape of a molecule plays a crucial role in its orientation within the cavity and its subsequent interaction potential, as previously mentioned.

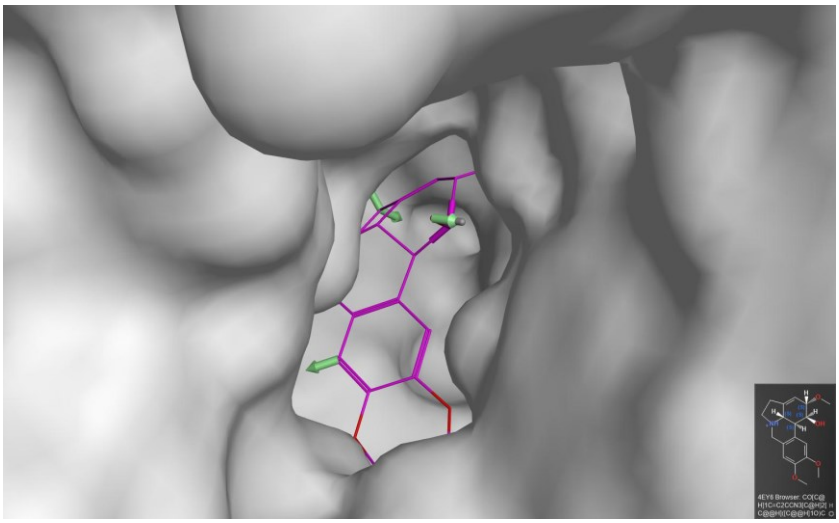

Figure 42. *Exit vectors of parent alkaloid* ***2****.*

Figure 42 describes an exit vector of **2**, indicating the direction in which the ligand is oriented within the binding site. The green arrows indicate the hydrogen atoms which can be substituted with at least methyl or larger substituent. As it is observable, one of the green arrows perfectly directs into the cavity tunnel, where our substituents have been added. Due to this good orientation and interaction potential, **2b** and **2d** fit well into the cavity (**Figure 43**, **Figure 44**).

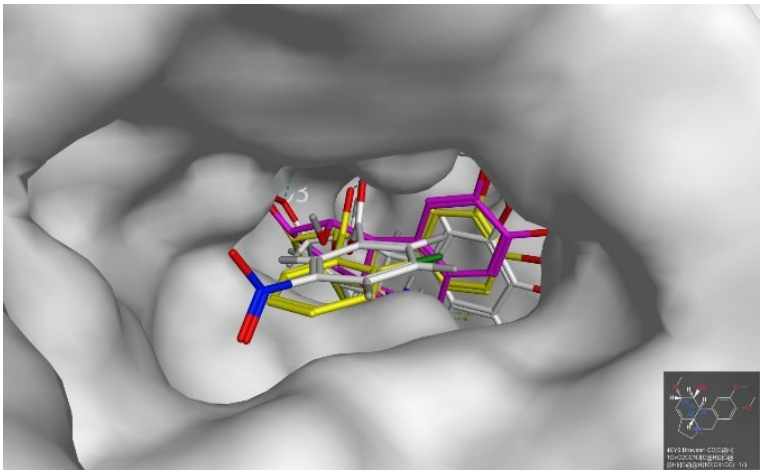

Figure 43. *Directing of derivatives to the cavity.tunnel Magenta = parent **2**; yellow: **2b**; white: **2d**.*

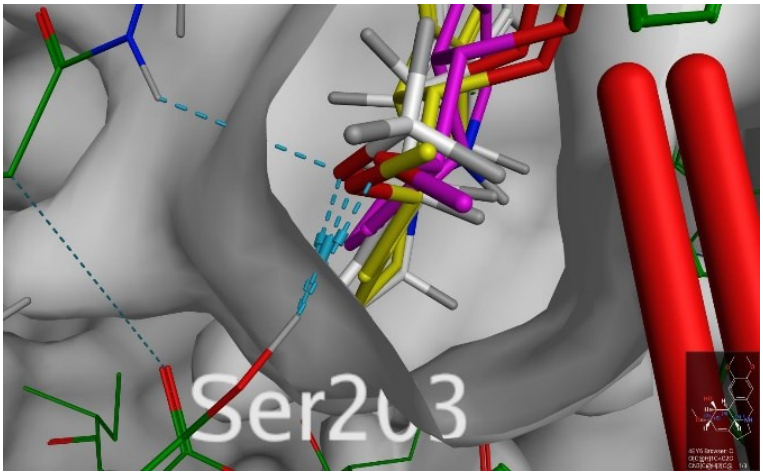

Figure 44. *Cross section of enzyme cavity in the area of the active site.*

In addition to the ideal fitting of the ligand to the cavity, the following interactions were shown (**Table 17**):

Table 17. *Comparison of interaction potentials of parent alkaloids and semisynthetic derivatives*

Alkaloid	Hydrogen bond residue	Aromatic interactions residue	Ion-dipole interaction residue	Dipole-dipole interaction residue	*h*AChE IC_{50} [μM]
2	Gly(121)/ Ser(203)				>10
2b	Ser(203), Tyr(124)	Trp(86)			>10
2d	Ser(203)	Trp(86)		Phe(295)	>10
4	Glu(202)	Gly(121), Phe(297), Trp(86)	Asp(74)		1.710 ± 0.065

Both derivatives exhibit specific interactions in the active site with Ser(203), as well as aromatic stabilizing interactions with Trp(86). Additionally, **2d** is characterized by a dipole-dipole interaction in the cavity tunnel with Phe(295), which can be considered a significant stabilizing interaction.

It is important to note that the enzyme used in our experiment is a rigid structure; however, in reality, the enzyme is dynamic and flexible. Amino acid residues can move and adjust to accommodate the ligand, leading to new interactions and potentially altering the binding site conformation. For this reason, the ligand-receptor complex generated by docking was refined using an unconstrained energic minimization for the **2**, **2b**, and **2d** ligands.

Table 18*. Comparison of modified enzymes interaction potentials*

Ligand	Interactions of the initial docked pose	Interactions after the unconstrained energetic minimization of the ligand-receptor complex
2b	Ser(203), Tyr(124), Trp(86)	Ser(203), Tyr(337), Trp(86), His(447)
2d	Ser(203), Trp(86), Phe(295)	Ser(203), His(447), Tyr(337), Trp(86), Phe(295)

Table 18 highlights that the enzyme is indeed a dynamic system. Both derivatives exhibit one additional interaction with His(447) in the active site after energetic minimization of the ligand-receptor complex. However, even this potential interaction does not guarantee biological activity (**Table 15**, **Table 17**).

In the literature, there are studies on **1**, which has been used as a scaffold for the synthesis of several lycorine derivatives with AChE inhibitory activity.[24] Compound **1** shares the same structural type as **2**, allowing us to compare the results of galanthine derivatives and draw inspiration. Notably, 1-acetoxy-2TBS-lycorine (Ki = 0.34 µM) and 1-benzoate-2-TBS-lycorine (Ki = 0.39 µM) exhibited good inhibitory activities, comparable with **4** (Ki = 0.30 µM), and are considered AChE potent inhibitors.[97]

This study highlights the positive effect of lipophilic substitution at C2 and polar H-bond acceptor groups at C1.[97] In comparison, our derivatives featured larger lipophilic substituents at C1 and methoxy group at C2. Despite achieving good orientation in the cavity and binding interactions, we did not observe significant in vitro inhibitory activity. The findings from the lycorine study could inspire further docking analysis, focusing on lipophilic derivatives at C2 and aiming to achieve the same good orientation in the cavity.

Comparison with donepezil

Donepezil, a registered substance from the group of AChE inhibitors, exhibits an IC_{50} = 1–10 nM. Although its chemical structure is entirely different from the scaffolds of Amaryllidaceae alkaloids described in this work, the molecular shape of donepezil and its fluor-derivative reveals some interesting similarities. For this comparison, enzymes 7E3H and 7D9P were used.

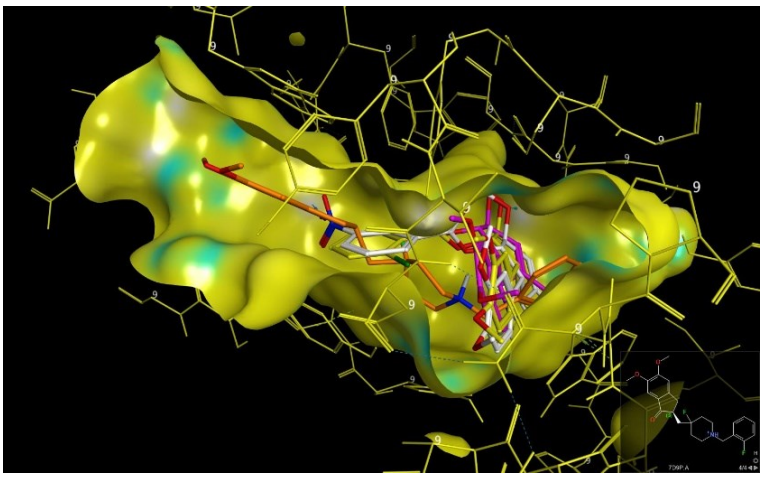

Figure 45. *Donepezil derivative (orange),* ***2*** *(cyclamen),* ***2b*** *(yellow) and* ***2d*** *(white) in the plastic cavity of hAChE crystallized with donepezil derivative (7D9P).*

From **Figure 45**, it is observable that the orientation of substituted benzyl derivatives of **2** and donepezil is similar within the tunnel of the enzyme cavity.

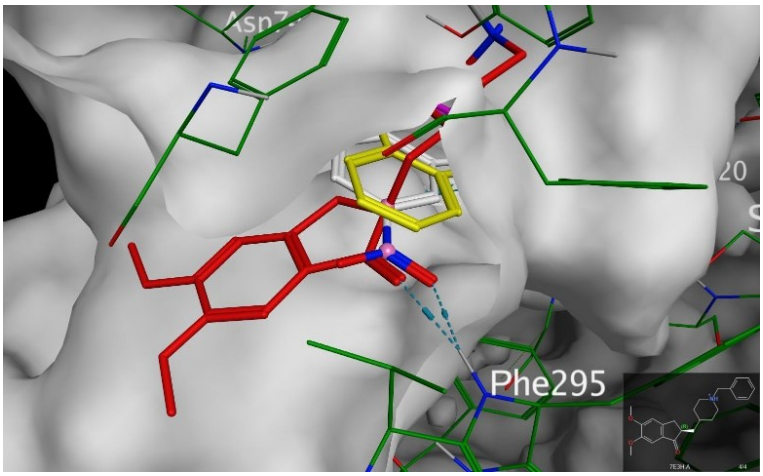

***Figure 46**. Interaction with Phe(295) in the cavity tunnel (7E3H).*

Significant interaction occurs with Phe(295) in the tunnel of the enzyme cavity, as previously described for **2d**. This observation may be crucial for the steric inhibition of the enzyme, which is stabilized by the dipole-dipole interaction of nitro group and phenylalanine in the tunnel.

Donepezil is well-known as a dual-binding site inhibitor, interacting simultaneously with the catalytic, peripheral, and mid-gorge binding sites, with documented interactions with Trp(86), Phe(295), and Trp(286).[98] However, **Figure 46** only shows interaction with Phe(295), because the molecular docking focused on the best position for binding interactions of galanthine derivatives, aiming to optimize the study of these derivatives rather than well-characterized donepezil. Nevertheless, the common interaction of **2d** and donepezil in the cavity tunnel provides inspiration for further study. Derivatives could be designed as dual-binding site inhibitors with a higher interaction potential in the catalytic site, thanks to the interaction potential of galanthine derivatives. It is also crucial to consider that inhibitors do not necessarily need to react with the catalytic site, they can also act as steric inhibitors. This opens possibilities for the substituents of the galanthine benzyl group, similar to the anacardic acid in Kiametis and co-workers (2017), which interacts with PAS residues and forms an anchor at the entrance.[99]

6 Conclusion

From 29 kg of fresh bulbs of *Narcissus poeticus* var. *recurvus,* 2.8 kg of summary extract was obtained, which was subsequently separated into 36.35 g of alkaloid extract. The alkaloid extract underwent GC/MS and HPLC/MS analysis, confirming the same results as those published in the initial screening study. Subsequently, the alkaloid extract was separated into 18 fractions and one acidic fraction by flash chromatography, and these fractions were again analysed using GC/MS and HPLC/MS. The fractions were then divided among the members of the research group for the isolation process.

During these plant material processing steps, the first alkaloid of this master's thesis was isolated. In particular, lycorine (6.2 g) precipitated during the LLE and was also crystallized in the tubes directly after flash chromatography separation.

This master's thesis focused next on fraction 8. From subfraction 8-4, galanthine (1.2 g), the major alkaloid of the fraction was isolated. From subfraction 8-2, cherylline (65.31 mg), the minor alkaloid was isolated.

All three alkaloids were structurally evaluated by mass spectrometry, NMR spectroscopy, and optical rotation, confirming that they were already known from the literature and that our results corresponded to those described in previous studies. Interesting observations were made regarding lycorine potential degradation, and the purification process was investigated. There is a suggestion for further stability study of lycorine and identification of possible degradation products or other impurities.

In vitro analysis was performed on all three alkaloids, including cytotoxicity screening for ten cell lines and inhibitory activity against human Topo IIα, indicating anticancer activity. Interesting results were obtained for cherylline anticancer activity against the MCF-7 cell line with prolonged exposition time or higher concentration, inspiring further study due to the good IC_{50} value (1.41 μM) obtained in the MTS assay.

To access alkaloid activity in the AD treatment, the alkaloids were tested for inhibitory potential against *h*AChE and *h*BuChE. In this Ellman's spectroscopy method, cherylline demonstrated good inhibition of *h*BuChE (IC_{50} = 11.34 ± 0.88 μM).

Molecular docking revealed interesting results for galanthine derivatives. Two derivatives, 2-chlorobenzoylgalanthine and 3-nitrobenzoylgalanthine, showed significant interactions and fit within the enzyme cavity. These findings inspire further study with substituents similar to those of donepezil, due to their similar fitting to the tunnel. Another promising direction for further research is focusing on lipophilic derivatives at C2.

Cherylline exhibited the most significant interactions among the isolated alkaloids. Although it did not show inhibition of *h*AChE, it remains an interesting scaffold for derivative studies.

In summary, this master's thesis accomplished its specific aims and contributed significantly to the broader phytochemical study. It laid the foundation for the phytochemical study by separating alkaloids into fractions and provided important results for the structurally known alkaloid cherylline, which is becoming an attractive subject for further research. Due to its lack of cytotoxicity for most cell lines (these results for nine new cell lines have not been published before) except for MCF-7, cherylline is a great candidate for studying *h*BuChE inhibition, which has gained interest in current studies. Additionally, it is a candidate for further biological testing against MCF-7, considering concentration and exposure time. Moreover, cherylline is a potential candidate for semisynthetic derivatives due to its good interaction potential in the enzyme observed in molecular docking and also for pharmacokinetic study. Furthermore, cherylline has been described in the study for its interesting biological activity in inhibiting the replication of Zika and Dengue viruses.[100] Even though cherylline was isolated as a minor alkaloid, some reports have indicated its presence not only in bulbs but also in leaves, which is another factor to consider for further research.[16]

Aside from cherylline, this work also provides a basis for further studies, including molecular docking to *h*BuChE, and hepatotoxicity tests for cherylline, which have not yet been described considering the history of tacrine.[101]

7 List of tables

8 List of figures

9 References

(1) Dias, D. A.; Urban, S.; Roessner, U. A Historical overview of natural products in drug discovery. *Metabolites* **2012**, *2* (2), 303–336. https://doi.org/10.3390/metabo2020303.

(2) Tzvetkov, N. T.; Kirilov, K.; Matin, M.; Atanasov, A. G. Natural product drug discovery and drug design: Two approaches shaping new pharmaceutical development. *Nephrol. Dial. Transplant.* **2024**, *39* (3), 375–378. https://doi.org/10.1093/ndt/gfad208.

(3) Velu, G.; Palanichamy, V.; Rajan, A. P. Phytochemical and pharmacological importance of plant secondary metabolites in modern medicine. In *Bioorganic phase in natural food: An overview*; Roopan, S. M., Madhumitha, G., Eds.; Springer International Publishing: Cham, **2018**; pp 135–156. https://doi.org/10.1007/978-3-319-74210-6_8.

(4) He, M.; Qu, C.; Gao, O.; Hu, X.; Hong, X. Biological and pharmacological activities of Amaryllidaceae alkaloids. *RSC Adv.* **2015**, *5* (21), 16562–16574. https://doi.org/10.1039/C4RA14666B.

(5) Evidente, A.; Kornienko, A. Anticancer evaluation of structurally diverse Amaryllidaceae alkaloids and their synthetic derivatives. *Phytochem. Rev.* **2009**, *8* (2), 449–459. https://doi.org/10.1007/s11101-008-9119-z.

(6) *Narcissus poeticus var. recurvus (Haw.) Herb. | Plants of the World Online | Kew Science*. Plants of the World Online. http://powo.science.kew.org/taxon/urn:lsid:ipni.org:names:311068-4 (accessed 2024-08-19).

(7) Cahlíková, L.; Benešová, N.; Macakova, K.; Kučera, R.; Hrstka, V.; Jahodár, L.; Opletal, L. Alkaloids from some Amaryllidaceae species and their cholinesterase activity. *Nat. Prod. Commun.* **2012**, *7*, 571–574. https://doi.org/10.1177/1934578X1200700506.

(8) Bastida, J.; Lavilla, R.; Viladomat, F. Chapter 3 Chemical and biological aspects of *Narcissus* alkaloids. In *The Alkaloids: Chemistry and biology*; Cordell, G. A., Ed.; Academic Press, **2006**; Vol. 63, pp 87–179. https://doi.org/10.1016/S1099-4831(06)63003-4.

(9) Hanks, G. R. *Narcissus and daffodil: The genus Narcissus*; CRC Press, **2002**.

(10) Compton, J. Haw. A Crisis of identity. *Curtiss Bot. Mag.* **2023**, *40* (2), 249–261. https://doi.org/10.1111/curt.12511.

(11) *RHS plant registration - Daffodil cultivars / RHS Gardening*. http://www.rhs.org.uk/plants/plantsmanship/plant-registration/daffodil-cultivar-registration (accessed 2024-08-01).

(12) s.r.o, L. G. *Narcis poeticus recurvus - narcissus, voňavý narcis - Lukon Glads s.r.o.* lukon-glads.cz. https://www.lukon-glads.cz/narcis-poeticus-recurvus/ (accessed 2024-08-01).

(13) Šafratová, M.; Hošťálková, A.; Hulcová, D.; Breiterová, K.; Hrabcová, V.; Machado, M.; Fontinha, D.; Prudêncio, M.; Kuneš, J.; Chlebek, J.; Jun, D.; Hrabinová, M.; Nováková, L.; Havelek, R.; Seifrtová, M.; Opletal, L.; Cahlíková, L. Alkaloids from *Narcissus poeticus* Cv. Pink Parasol of various structural types and their biological activity. *Arch. Pharm. Res.* **2018**, *41* (2), 208–218. https://doi.org/10.1007/s12272-017-1000-4.

(14) Ločárek, M.; Novakova Kocendova, J.; Kloucek, P.; Hošťálková, A.; Kokoska, L.; Gábrlová, L.; Safratova, M.; Opletal, L.; Cahlíková, L. Antifungal and antibacterial activity of extracts and alkaloids of selected Amaryllidaceae species. *Nat. Prod. Commun.* **2015**, *10*, 1537–1540. https://doi.org/10.1177/1934578X1501000912.

(15) Pustahija, F.; Bašić, N.; Siljak-Yakovlev, S. Karyotype variability in wild *Narcissus Poeticus* L. populations from different environmental conditions in the Dinaric Alps. *Plants* **2024**, *13* (2), 208. https://doi.org/10.3390/plants13020208.

(16) Torras-Claveria, L.; Berkov, S.; Codina, C.; Viladomat, F.; Bastida, J. Metabolomic analysis of bioactive Amaryllidaceae alkaloids of ornamental varieties of *Narcissus* by GC–MS combined with k-Means cluster analysis. *Ind. Crops Prod.* **2014**, *56*, 211–222. https://doi.org/10.1016/j.indcrop.2014.03.008.

(17) Heinrich, M.; Lee Teoh, H. Galanthamine from snowdrop—the development of a modern drug against Alzheimer's disease from local Caucasian knowledge. *J. Ethnopharmacol.* **2004**, *92* (2), 147–162. https://doi.org/10.1016/j.jep.2004.02.012.
(18) Kalola, U. K.; Patel, P.; Nguyen, H. Galantamine. In *StatPearls*; StatPearls Publishing: Treasure Island (FL), **2024**.
(19) Berkov, S.; Georgieva, L.; Kondakova, V.; Atanassov, A.; Viladomat, F.; Bastida, J.; Codina, C. Plant sources of galanthamine: Phytochemical and biotechnological aspects. *Biotechnol. Biotechnol. Equip.* **2009**, *23* (2), 1170–1176. https://doi.org/10.1080/13102818.2009.10817633.
(20) Pyke, N.; Stephens, K.; McLeod, M.; Glare, T.; Narciso, J. *Daffodil production for galanthamine*; report; AgResearch, **2023**. https://doi.org/10.57935/AGR.26001694.v1.
(21) Miller, I. R.; McLean, N. J.; Moustafa, G. A. I.; Ajavakom, V.; Kemp, S. C.; Bellingham, R. K.; Camp, N. P.; Brown, R. C. D. Transition-metal-mediated chemo- and stereoselective total synthesis of (−)-galanthamine. *J. Org. Chem.* **2022**, *87* (2), 1325–1334. https://doi.org/10.1021/acs.joc.1c02638.
(22) Majumder, S.; Yadav, A.; Souvik, P.; Bisai, A. Asymmetric total syntheses of (−)-lycoramine, (−)-lycoraminone, (−)-narwedine, and (−)-galanthamine. *J. Org. Chem.* **2022**, *87* (12), 7786–7797. https://doi.org/10.1021/acs.joc.2c00420.
(23) Sanyal, R.; M., M.; Pandey, S.; Nandi, S.; Biswas, P.; Dewanjee, S.; Gopalakrishnan, A. V.; Jha, N. K.; Jha, S. K.; Joshee, N.; Pandey, D. K.; Dey, A.; Shekhawat, M. S. Biotechnological interventions and production of galanthamine in *Crinum* spp. *Appl. Microbiol. Biotechnol.* **2023**, *107* (7), 2155–2167. https://doi.org/10.1007/s00253-023-12444-0.
(24) Berkov, S.; Atanasova, M.; Georgiev, B.; Bastida, J.; Doytchinova, I. The Amaryllidaceae alkaloids: An untapped source of acetylcholinesterase inhibitors. *Phytochem. Rev.* **2022**, *21* (5), 1415–1443. https://doi.org/10.1007/s11101-021-09790-0.
(25) Bednářik, J.; Ambler, Z.; Růžička, E.; et. al. *Klinická neurologie, část speciální I*; TRITON: Praha, **2010**.
(26) Scheltens, P.; Strooper, B. D.; Kivipelto, M.; Holstege, H.; Chételat, G.; Teunissen, C. E.; Cummings, J.; van der Flier, W. M. Alzheimer's disease. *Lancet Lond. Engl.* **2021**, *397* (10284), 1577–1590. https://doi.org/10.1016/S0140-6736(20)32205-4.
(27) Nasb, M.; Tao, W.; Chen, N. Alzheimer's disease puzzle: Delving into pathogenesis hypotheses. *Aging Dis.* **2024**, *15* (1), 43–73. https://doi.org/10.14336/AD.2023.0608.
(28) Khan, S.; Barve, K. H.; Kumar, M. S. Recent advancements in pathogenesis, diagnostics and treatment of Alzheimer's disease. *Curr. Neuropharmacol.* **2020**, *18* (11), 1106–1125. https://doi.org/10.2174/1570159X18666200528142429.
(29) Uhrová, T.; Roth, J.; et. al. *Neuropsychiatrie. Klinický průvodce pro ambulantní i nemocniční praxi.*; Maxdorf: Praha, **2020.**
(30) Loof, A. D.; Schoofs, L. Alzheimer's disease: is a dysfunctional mevalonate biosynthetic pathway the master-inducer of deleterious changes in cell physiology? *OBM Neurobiol.* **2019**, *3* (4), 1–1. https://doi.org/10.21926/obm.neurobiol.1904046.
(31) Yan, Y.-P.; Chen, J.-Y.; Lu, J.-H. Disease-modifying activity of huperzine A on Alzheimer's disease: Evidence from preclinical studies on rodent models. *Int. J. Mol. Sci.* **2022**, *23* (23), 15238. https://doi.org/10.3390/ijms232315238.
(32) Alhazmi, H. A.; Albratty, M. An update on the novel and approved drugs for Alzheimer disease. *Saudi Pharm. J.* **2022**, *30* (12), 1755–1764. https://doi.org/10.1016/j.jsps.2022.10.004.
(33) Padda, I. S.; Parmar, M. Aducanumab. In *StatPearls*; StatPearls Publishing: Treasure Island (FL), 2024.
(34) European Medicines Agency rejects marketing authorisation application for aducanumab. https://www.alzheimer-europe.org/news/european-medicines-agency-rejects-marketing-authorisation-application-aducanumab?language_content_entity=en (accessed 2024-08-28)
(35) Chowdhury, S.; Chowdhury, N. S. Novel anti-amyloid-beta (Aβ) monoclonal antibody lecanemab for Alzheimer's disease: A systematic review. *Int. J. Immunopathol. Pharmacol.* **2023**, *37*, 03946320231209839. https://doi.org/10.1177/03946320231209839.

(36) *Leqembi | European Medicines Agency (EMA)*. https://www.ema.europa.eu/en/medicines/human/EPAR/leqembi (accessed 2024-08-28).
(37) Breijyeh, Z.; Karaman, R. Comprehensive review on Alzheimer's disease: Causes and treatment. *Molecules* **2020**, *25* (24), 5789. https://doi.org/10.3390/molecules25245789.
(38) Hampel, H.; Mesulam, M.-M.; Cuello, A. C.; Farlow, M. R.; Giacobini, E.; Grossberg, G. T.; Khachaturian, A. S.; Vergallo, A.; Cavedo, E.; Snyder, P. J.; Khachaturian, Z. S. The cholinergic system in the pathophysiology and treatment of Alzheimer's disease. *Brain* **2018**, *141* (7), 1917–1933. https://doi.org/10.1093/brain/awy132.
(39) Silva, T.; Reis, J.; Teixeira, J.; Borges, F. Alzheimer's disease, enzyme targets and drug discovery struggles: From natural products to drug prototypes. *Ageing Res. Rev.* **2014**, *15*, 116–145. https://doi.org/10.1016/j.arr.2014.03.008.
(40) Cahlíková, L.; Vrabec, R.; Pidaný, F.; Peřinová, R.; Maafi, N.; Mamun, A. A.; Ritomská, A.; Wijaya, V.; Blunden, G. Recent progress on biological activity of Amaryllidaceae and further isoquinoline alkaloids in connection with Alzheimer's disease. *Molecules* **2021**, *26* (17), 5240. https://doi.org/10.3390/molecules26175240.
(41) Sridhar, G. R.; Gumpeny, L. Emerging significance of butyrylcholinesterase. *World J. Exp. Med.* **2024**, *14* (1), 87202. https://doi.org/10.5493/wjem.v14.i1.87202.
(42) Gottwald, M. D.; Rozanski, R. I. Rivastigmine, a brain-region selective acetylcholinesterase inhibitor for treating Alzheimer's disease: Review and current status. *Expert Opin. Investig. Drugs* **1999**, *8* (10), 1673–1682. https://doi.org/10.1517/13543784.8.10.1673.
(43) Cimmino, A.; Masi, M.; Evidente, M.; Superchi, S.; Evidente, A. Amaryllidaceae alkaloids: Absolute configuration and biological activity. *Chirality* **2017**, *29* (9), 486–499. https://doi.org/10.1002/chir.22719.
(44) Nair, J. J.; Rárová, L.; Strnad, M.; Bastida, J.; van Staden, J. Mechanistic insights to the cytotoxicity of Amaryllidaceae alkaloids. *Nat. Prod. Commun.* **2015**, *10* (1), 1934578X1501000138. https://doi.org/10.1177/1934578X1501000138.
(45) Roy, M.; Liang, L.; Xiao, X.; Feng, P.; Ye, M.; Liu, J. Lycorine: A prospective natural lead for anticancer drug discovery. *Biomed. Pharmacother.* **2018**, *107*, 615–624. https://doi.org/10.1016/j.biopha.2018.07.147.
(46) Khalifa, M.; Attia, E.; Fahim, J.; Kamel, M. An Overview on the chemical and biological aspects of lycorine alkaloid. *J. Adv. Biomed. Pharm. Sci.* **2018**, *1* (2), 41–49. https://doi.org/10.21608/jabps.2018.4088.1016.
(47) Lamoral-Theys, D.; Andolfi, A.; Van Goietsenoven, G.; Cimmino, A.; Le Calvé, B.; Wauthoz, N.; Mégalizzi, V.; Gras, T.; Bruyère, C.; Dubois, J.; Mathieu, V.; Kornienko, A.; Kiss, R.; Evidente, A. Lycorine, the main phenanthridine Amaryllidaceae alkaloid, exhibits significant antitumor activity in cancer cells that display resistance to proapoptotic stimuli: An investigation of structure−activity relationship and mechanistic insight. *J. Med. Chem.* **2009**, *52* (20), 6244–6256. https://doi.org/10.1021/jm901031h.
(48) Katoch, D.; Kumar, D.; Sharma, U.; Kumar, N.; Padwad, Y. S.; Lal, B.; Singh, B. Zephgrabetaine: A new betaine-type Amaryllidaceae alkaloid from *Zephyranthes grandiflora*. *Nat. Prod. Commun.* **2013**, *8* (2), 1934578X1300800206. https://doi.org/10.1177/1934578X1300800206.
(49) Wang, P.; Yuan, H.-H.; Zhang, X.; Li, Y.-P.; Shang, L.-Q.; Yin, Z. Novel lycorine derivatives as anticancer agents: Synthesis and *in vitro* biological evaluation. *Molecules* **2014**, *19* (2), 2469–2480. https://doi.org/10.3390/molecules19022469.
(50) Nair, J. J.; Van Staden, J.; Bastida, J. Chapter 3 - Cytotoxic alkaloid constituents of the Amaryllidaceae. In *Studies in Natural Products Chemistry*; Atta-ur-Rahman, Ed.; Elsevier, 2016; Vol. 49, pp 107–156. https://doi.org/10.1016/B978-0-444-63601-0.00003-X.
(51) Lamoral-Theys, D.; Decaestecker, C.; Mathieu, V.; Dubois, J.; Kornienko, A.; Kiss, R.; Evidente, A.; Pottier, L. Lycorine and its derivatives for anticancer drug design. *Mini Rev. Med. Chem.* **2010**, *10* (1), 41–50. https://doi.org/10.2174/138955710791112604.

(52) Habartová, K.; Cahlíková, L.; Řezáčová, M.; Havelek, R. The biological activity of alkaloids from the Amaryllidaceae: From cholinesterases inhibition to anticancer activity. *Nat. Prod. Commun.* **2016**, *11* (10), 1934578X1601101038. https://doi.org/10.1177/1934578X1601101038.
(53) Liu, J.; Sun, S.; Zhou, C.; Sun, Z.; Wang, Q.; Sun, C. *In vitro* and *in vivo* anticancer activity of lycorine in prostate cancer by inhibiting NF-κB signaling pathway. *J. Cancer* **2022**, *13* (10), 3151–3159. https://doi.org/10.7150/jca.75597.
(54) Cahlíková, L.; Kawano, I.; Řezáčová, M.; Blunden, G.; Hulcová, D.; Havelek, R. The Amaryllidaceae alkaloids haemanthamine, haemanthidine and their semisynthetic derivatives as potential drugs. *Phytochem. Rev.* **2021**, *20* (1), 303–323. https://doi.org/10.1007/s11101-020-09675-8.
(55) Hroch, M.; Mičuda, S.; Havelek, R.; Cermanová, J.; Cahlíková, L.; Hošťálková, A.; Hulcová, D.; Řezáčová, M. LC-MS/MS Method for the determination of haemanthamine in rat plasma, bile and urine and its application to a pilot pharmacokinetic study. *Biomed. Chromatogr.* **2016**, *30* (7), 1083–1091. https://doi.org/10.1002/bmc.3653.
(56) Cedrón, J. C.; Ravelo, Á. G.; León, L. G.; Padrón, J. M.; Estévez-Braun, A. Antiproliferative and structure activity relationships of Amaryllidaceae alkaloids. *Molecules* **2015**, *20* (8), 13854–13863. https://doi.org/10.3390/molecules200813854.
(57) Nair, J. J.; van Staden, J. Cell cycle modulatory effects of Amaryllidaceae alkaloids. *Life Sci.* **2018**, *213*, 94–101. https://doi.org/10.1016/j.lfs.2018.08.073.
(58) Wang, M.; Liang, L.; Wang, R.; Jia, S.; Xu, C.; Wang, Y.; Luo, M.; Lin, Q.; Yang, M.; Zhou, H.; Liu, D.; Qing, C. Narciclasine, a novel topoisomerase I inhibitor, exhibited potent anti-cancer activity against cancer cells. *Nat. Prod. Bioprospecting* **2023**, *13* (1), 27. https://doi.org/10.1007/s13659-023-00392-1.
(59) Ingrassia, L.; Lefranc, F.; Dewelle, J.; Pottier, L.; Mathieu, V.; Spiegl-Kreinecker, S.; Sauvage, S.; El Yazidi, M.; Dehoux, M.; Berger, W.; Van Quaquebeke, E.; Kiss, R. Structure−activity relationship analysis of novel derivatives of narciclasine (an Amaryllidaceae isocarbostyril derivative) as potential anticancer agents. *J. Med. Chem.* **2009**, *52* (4), 1100–1114. https://doi.org/10.1021/jm8013585.
(60) Ma, D.; Pignanelli, C.; Tarade, D.; Gilbert, T.; Noel, M.; Mansour, F.; Adams, S.; Dowhayko, A.; Stokes, K.; Vshyvenko, S.; Collins, J.; Hudlicky, T.; McNulty, J.; Pandey, S. Cancer cell mitochondria targeting by pancratistatin analogs is dependent on functional complex II and III. *Sci. Rep.* **2017**, *7* (1), 42957. https://doi.org/10.1038/srep42957.
(61) Koutová, D.; Maafi, N.; Havelek, R.; Opletal, L.; Blunden, G.; Řezáčová, M.; Cahlíková, L. Chemical and biological aspects of montanine-type alkaloids isolated from plants of the Amaryllidaceae family. *Molecules* **2020**, *25* (10), 2337. https://doi.org/10.3390/molecules25102337.
(62) Munier, R. Separation of alkaloids from their N-oxides by paper chromatography. *Bull Soc Chim Biol* **1953**, *35* (1225).
(63) *Československý Lékopis*, 3.; Avicenum: Praha, 1971; Vol. I.
(64) Hrabinova, M.; Pejchal, J.; Hepnarova, V.; Muckova, L.; Junova, L.; et. al. A-Series Agent A-234: Initial *in vitro* and *in vivo* characterization. *Arch. Toxicol.* **2024**, *98* (4). https://doi.org/10.1007/s00204-024-03689-3.
(65) Ellman, G. L.; Courtney, K. D.; Andres, V.; Featherstone, R. M. A new and rapid colorimetric determination of acetylcholinesterase activity. *Biochem. Pharmacol.* **1961**, *7* (2), 88–95. https://doi.org/10.1016/0006-2952(61)90145-9.
(66) Dernovšek, J.; Zajec, Ž.; Durcik, M.; Mašič, L. P.; Gobec, M.; Zidar, N.; Tomašič, T. Structure-activity relationships of benzothiazole-based Hsp90 C-terminal-domain inhibitors. *Pharmaceutics* **2021**, *13* (8), 1283. https://doi.org/10.3390/pharmaceutics13081283.
(67) Lojkásek, M. Izolace alkaloidu galanthinu z *Narcissus poeticus recurvus* a jeho polosyntetické deriváty. Master's thesis. Charles University, Faculty of Pharmacy in Hradec Králové, **2023**.
(68) Mondy, N.; Naudin, A.; Christides, J. P.; Mandon, N.; Auger, J. Comparison of GC-MS and HPLC for the analysis of *Allium* volatiles. *Chromatographia* **2001**, *53* (1), S356–S360. https://doi.org/10.1007/BF02490356.

(69) Yu, H.; Du, B.; Qiu, Y.; Wang, T.; Zhou, S.; Han, L.; Liu, E.; Chen, L. Preparation for improving water dispersibility of lycorine, prolonging half-life period of lycorine and improving antitumor activity of lycorine and application of preparation. CN113350292A, September 7, **2021.**
(70) Kozikowski, B. A.; Burt, T. M.; Tirey, D. A.; Williams, L. E.; Kuzmak, B. R.; Stanton, D. T.; Morand, K. L.; Nelson, S. L. The effect of room-temperature storage on the stability of compounds in DMSO. *SLAS Discov.* **2003**, *8* (2), 205–209. https://doi.org/10.1177/1087057103252617.
(71) Cook, J. W.; Loudon, J. D. Chapter XI Alkaloids of the Amaryllidaceae. In *The Alkaloids: Chemistry and Physiology*; Manske, R. H. F., Holmes, H. L., Eds.; The Alkaloids Chemistry and Physiology; Academic Press, **1952**; Vol. 2, pp 331–352. https://doi.org/10.1016/S1876-0813(08)60028-7.
(72) Pannequin, A.; Laurini, E.; Giordano, L.; Muselli, A.; Pricl, S.; Tintaru, A. Caution: Chemical instability of natural biomolecules during routine analysis. *Molecules* **2020**, *25* (14), 3292. https://doi.org/10.3390/molecules25143292.
(73) Maltese, F.; van der Kooy, F.; Verpoorte, R. Solvent derived artifacts in natural products chemistry. *Nat. Prod. Commun.* **2009**, *4* (3), 447–454.
(74) Bastida, J.; Codina, C.; Viladomat, F.; Rubiralta, M.; Quirion, J.-C.; Husson, H.-P.; Ma, G. *Narcissus* alkaloids, XIII. Complete assignment of the Nmr spectra of papyramine and 6-epi-papyramine by two-dimensional Nmr spectroscopy. *J. Nat. Prod.* **1990**, *53* (6), 1456–1462. https://doi.org/10.1021/np50072a009.
(75) Lebrun, S.; Couture, A.; Deniau, E.; Grandclaudon, P. A new synthesis of (+)- and (−)-cherylline. *Org. Biomol. Chem.* **2003**, *1* (10), 1701–1706. https://doi.org/10.1039/B302168H.
(76) Cao, Z.; Yang, P.; Zhou, Q. Multiple biological functions and pharmacological effects of lycorine. *Sci. China Chem.* **2013**, *56* (10), 1382–1391. https://doi.org/10.1007/s11426-013-4967-9.
(77) Ka, S.; Masi, M.; Merindol, N.; Di Lecce, R.; Plourde, M. B.; Seck, M.; Górecki, M.; Pescitelli, G.; Desgagne-Penix, I.; Evidente, A. Gigantelline, gigantellinine and gigancrinine, cherylline- and crinine-type alkaloids isolated from *Crinum Jagus* with anti-acetylcholinesterase activity. *Phytochemistry* **2020**, *175*, 112390. https://doi.org/10.1016/j.phytochem.2020.112390.
(78) Hulcová, D.; Maříková, J.; Korábečný, J.; Hošťálková, A.; Jun, D.; Kuneš, J.; Chlebek, J.; Opletal, L.; De Simone, A.; Nováková, L.; Andrisano, V.; Růžička, A.; Cahlíková, L. Amaryllidaceae alkaloids from *Narcissus Pseudonarcissus* L. Cv. Dutch Master as potential drugs in treatment of Alzheimer's disease. *Phytochemistry* **2019**, *165*, 112055. https://doi.org/10.1016/j.phytochem.2019.112055.
(79) Sierra, K.; de Andrade, J. P.; R. Tallini, L.; Osorio, E. H.; Yañéz, O.; Osorio, M. I.; Oleas, N. H.; García-Beltrán, O.; de S. Borges, W.; Bastida, J.; Osorio, E.; Cortes, N. *In vitro* and *in silico* analysis of galanthine from *Zephyranthes Carinata* as an inhibitor of acetylcholinesterase. *Biomed. Pharmacother.* **2022**, *150*, 113016. https://doi.org/10.1016/j.biopha.2022.113016.
(80) Cahlíková, L.; Breiterová, K.; Opletal, L. Chemistry and biological activity of alkaloids from the genus *Lycoris* (Amaryllidaceae). *Molecules* **2020**, *25* (20), 4797. https://doi.org/10.3390/molecules25204797.
(81) Wang, Y.-H.; Wan, Q.-L.; Gu, C.-D.; Luo, H.-R.; Long, C.-L. Synthesis and biological evaluation of lycorine derivatives as dual inhibitors of humanacetylcholinesterase and butyrylcholinesterase. *Chem. Cent. J.* **2012**, *6* (1), 96. https://doi.org/10.1186/1752-153X-6-96.
(82) Evidente, A. Advances on the Amaryllidaceae alkaloids collected in South Africa, Andean South America and the Mediterranean Basin. *Molecules* **2023**, *28* (10), 4055. https://doi.org/10.3390/molecules28104055.
(83) Havelek, R.; Muthna, D.; Tomsik, P.; Kralovec, K.; Seifrtova, M.; Cahlikova, L.; Hostalkova, A.; Safratova, M.; Perwein, M.; Cermakova, E.; Rezacova, M. Anticancer potential of Amaryllidaceae alkaloids evaluated by screening with a panel of human cells, real-time cellular analysis and Ehrlich tumor-bearing mice. *Chem. Biol. Interact.* **2017**, *275*, 121–132. https://doi.org/10.1016/j.cbi.2017.07.018.
(84) Nair, J. J.; van Staden, J. Cytotoxicity studies of lycorine alkaloids of the Amaryllidaceae. *Nat. Prod. Commun.* **2014**, *9* (8), 1193–1210.

(85) Van Goietsenoven, G.; Andolfi, A.; Lallemand, B.; Cimmino, A.; Lamoral-Theys, D.; Gras, T.; Abou-Donia, A.; Dubois, J.; Lefranc, F.; Mathieu, V.; Kornienko, A.; Kiss, R.; Evidente, A. Amaryllidaceae alkaloids belonging to different structural subgroups display activity against apoptosis-resistant cancer cells. *J. Nat. Prod.* **2010**, *73* (7), 1223–1227. https://doi.org/10.1021/np9008255.

(86) Riss, T.; Niles, A.; Moravec, R.; Karassina, N.; Vidugiriene, J.; et. al. Cytotoxicity assays: *in vitro* methods to measure dead cells. In *Assay Guidance Manual*; Eli Lilly & Company and the National Center for Advancing Translational Sciences: Bethesda (MD), **2004.**

(87) Ji, Y.; Yu, M.; Qi, Z.; Cui, D.; Xin, G.; Wang, B.; Jia, W.; Chang, L. Study on apoptosis effect of human breast cancer cell MCF-7 induced by lycorine hydrochloride via death receptor pathway. *Saudi Pharm. J.* **2017**, *25* (4), 633–637. https://doi.org/10.1016/j.jsps.2017.04.036.

(88) Tallini, L. R.; Machado das Neves, G.; Vendruscolo, M. H.; Rezende-Teixeira, P.; Borges, W.; Bastida, J.; Costa-Lotufo, L. V.; Eifler-Lima, V. L.; Zuanazzi, J. A. S. Antitumoral activity of different Amaryllidaceae alkaloids: *In vitro* and *in silico* assays. *J. Ethnopharmacol.* **2024**, *329*, 118154. https://doi.org/10.1016/j.jep.2024.118154.

(89) Niño, J.; Hincapié, G.; Correa, Y.; Mosquera, O. Alkaloids of *Crinum x powellii* "album" (Amaryllidaceae) and their topoisomerase inhibitory activity. *Z. Für Naturforschung C J. Biosci.* **2014**, *62*, 223–226. https://doi.org/10.1515/znc-2007-3-411.

(90) Asiamah, I.; Obiri, S. A.; Tamekloe, W.; Armah, F. A.; Borquaye, L. S. Applications of molecular docking in natural products-based drug discovery. *Sci. Afr.* **2023**, *20*, e01593. https://doi.org/10.1016/j.sciaf.2023.e01593.

(91) Dvir, H.; Silman, I.; Harel, M.; Rosenberry, T. L.; Sussman, J. L. Acetylcholinesterase: from 3D structure to function. *Chem. Biol. Interact.* **2010**, *187* (1–3), 10–22. https://doi.org/10.1016/j.cbi.2010.01.042.

(92) Silva, L. B.; Ferreira, E. F. B.; Maryam; Espejo-Román, J. M.; Costa, G. V.; Cruz, J. V.; Kimani, N. M.; Costa, J. S.; Bittencourt, J. A. H. M.; Cruz, J. N.; Campos, J. M.; Santos, C. B. R. Galantamine based novel acetylcholinesterase enzyme inhibitors: A molecular modeling design approach. *Molecules* **2023**, *28* (3), 1035. https://doi.org/10.3390/molecules28031035.

(93) López, A. F. F.; Martínez, O. M. M.; Hernández, H. F. C. Evaluation of *Amaryllidaceae* alkaloids as inhibitors of human acetylcholinesterase by QSAR analysis and molecular docking. *J. Mol. Struct.* **2021**, *1225*, 129142. https://doi.org/10.1016/j.molstruc.2020.129142.

(94) Pelkonen, O.; Turpeinen, M.; Raunio, H. *In vivo-in vitro-in silico* pharmacokinetic modelling in drug development. *Clin. Pharmacokinet.* **2011**, *50* (8), 483–491. https://doi.org/10.2165/11592400-000000000-00000.

(95) Stavrakov, G.; Philipova, I.; Lukarski, A.; Atanasova, M.; Georgiev, B.; Atanasova, T.; Konstantinov, S.; Doytchinova, I. Discovery of a novel acetylcholinesterase inhibitor by fragment-based design and virtual screening. *Mol. Basel Switz.* **2021**, *26* (7), 2058. https://doi.org/10.3390/molecules26072058.

(96) Atanasova, M.; Yordanov, N.; Dimitrov, I.; Berkov, S.; Doytchinova, I. Molecular docking study on galantamine derivatives as cholinesterase inhibitors. *Mol. Inform.* **2015**, *34* (6–7), 394–403. https://doi.org/10.1002/minf.201400145.

(97) McNulty, J.; Nair, J. J.; Little, J. R. L.; Brennan, J. D.; Bastida, J. Structure–activity studies on acetylcholinesterase inhibition in the lycorine series of Amaryllidaceae alkaloids. *Bioorg. Med. Chem. Lett.* **2010**, *20* (17), 5290–5294. https://doi.org/10.1016/j.bmcl.2010.06.130.

(98) Borges, N. M.; Sartori, G. R.; Ribeiro, J. F. R.; Rocha, J. R.; Martins, J. B. L.; Montanari, C. A.; Gargano, R. Similarity search combined with docking and molecular dynamics for novel *h*AChE inhibitor scaffolds. *J. Mol. Model.* **2018**, *24* (1), 41. https://doi.org/10.1007/s00894-017-3548-9.

(99) Kiametis, A. S.; Silva, M. A.; Romeiro, L. A. S.; Martins, J. B. L.; Gargano, R. Potential acetylcholinesterase inhibitors: Molecular docking, molecular dynamics, and *in silico* prediction. *J. Mol. Model.* **2017**, *23* (2), 67. https://doi.org/10.1007/s00894-017-3228-9.

(100) Ka, S.; Merindol, N.; Sow, A. A.; Singh, A.; Landelouci, K.; Plourde, M. B.; Pépin, G.; Masi, M.; Di Lecce, R.; Evidente, A.; Seck, M.; Berthoux, L.; Chatel-Chaix, L.; Desgagné-Penix, I.

Amaryllidaceae alkaloid cherylline inhibits the replication of Dengue and Zika viruses. *Antimicrob. Agents Chemother.* **2021**, *65* (9), 10.1128/aac.00398-21. https://doi.org/10.1128/aac.00398-21.

(101) Watkins, P. B.; Zimmerman, H. J.; Knapp, M. J.; Gracon, S. I.; Lewis, K. W. Hepatotoxic effects of tacrine administration in patients with Alzheimer's disease. *JAMA* **1994**, *271* (13), 992–998.

10 Abstract

Charles University, Faculty of Pharmacy in Hradec Králové

Department of Pharmacognosy and Pharmaceutical Botany

Candidate: Simona Hašanová

Supervisor: PharmDr. Daniela Suchánková, Ph.D.

Consultant: PharmDr. Jana Křoustková, Ph.D.

Title: Amaryllidaceae alkaloids of *Narcissus poeticus* var. *recurvus* and their implication to Alzheimer's disease and anticancer activity

Keywords: Amaryllidaceae alkaloids, separation, isolation, lycorine, cherylline, galanthine, cholinesterase-inhibitory activity, cytotoxicity, *in silico* study

An extensive phytochemical study was carried out on 29 kg of fresh bulbs of *Narcissus poeticus* var. *recurvus* based on preliminary results of the effects of alkaloid extract on *h*AChE and *h*BuChE. By processing the plant material, 36.4 g of alkaloidal extract was obtained, which was subsequently separated into 18 fractions by flash chromatography. The most abundant alkaloid in this plant, lycorine, was directly precipitated from the solution in a yield of 6.2 g. However, this thesis further focused on the processing of fraction 8, out of which two other alkaloids were obtained, namely galanthine (1.2 g) and cherylline (65.3 mg). MS, NMR analyses, and specific rotation elucidated the structures of all three alkaloids. Therefore, since Amaryllidaceae alkaloids are known biologically active compounds, three isolated compounds were subjected to *in vitro* analysis of *h*AChE/*h*BuChE inhibition activity and cytotoxicity screening (Jurkat, MOLT-4, A549, HT-29, PANC-1, A2780, SHSY5Y, MCF-7, SAOS-2, MRC-5 cell line, and human topoisomerase IIα). Cherylline exhibited good inhibitory activity against *h*BuChE, while was presented as no cytotoxic, and interesting results were observed for the MCF-7 cell line. In addition, *h*AChE activity was the subject of an *in silico* study to identify the interaction sites between the chemical scaffold and the enzymatic amino acid residues of isolated alkaloids.

11 Abstrakt

Univerzita Karlova, Farmaceutická fakulta v Hradci Králové

Katedra farmakognozie a farmaceutické botaniky

Riešiteľ: Simona Hašanová

Školiteľ: PharmDr. Daniela Suchánková, Ph.D.

Konzultant: PharmDr. Jana Křoustková, Ph.D.

Názov: Amarylkovité alkaloidy z *Narcissus poeticus* var. *recurvus* a ich implikácia v Alzheimerovej chorobe a protinádorovej aktivite

Kľúčové slová: Amarylkovité alkaloidy, separácia, izolácia, lykorín, cherylín, galantín, cholínesterázová inhibičná aktivita, cytotoxicita, *in silico* štúdia.

Na 29 kg čerstvých cibúľ druhu *Narcissus poeticus* var. *recurvus* bola zrealizovaná rozsiahla fytochemická štúdia na základe predbežných výsledkov alkaloidného extraktu na *h*AChE a *h*BuChE. Spracovaním rastlinného materiálu sa získalo 36,4 g alkaloidného extraktu, ktorý bol následne rozdelený na 18 frakcií pomocou flash chromatografie. Najzastúpenejší alkaloid v tejto rastline, lykorín, sa priamo precipitoval z roztoku s výťažkom 6,2 g. Avšak, táto diplomová práca sa ďalej zamerala na spracovanie frakcie 8, z ktorej boli získané ďalšie dva alkaloidy, konkrétne galantín (1,2 g) a cherylín (65,3 mg). Štruktúry všetkých troch alkaloidov boli objasnené pomocou MS, NMR analýz a merania špecifickej rotácie. Keďže alkaloidy z čeľade Amaryllidaceae sú známe biologicky aktívne látky, tri izolované zlúčeniny boli podrobené *in vitro* analýze inhibičnej aktivity na *h*AChE/*h*BuChE a skríningu cytotoxicity (bunkové línie: Jurkat, MOLT-4, A549, HT-29, PANC-1, A2780, SHSY5Y, MCF-7, SAOS-2, MRC-5 a ľudská topoizomeráza IIα). Cherylín preukázal dobrú inhibičnú aktivitu voči *h*BuChE, zatiaľ čo nepreukázal cytotoxicitu, pričom zaujímavé výsledky boli pozorované pri bunkovej línii MCF-7. Okrem toho bola aktivita *h*AChE predmetom *in silico* štúdie s cieľom identifikovať interakčné miesta medzi chemickým základom a aminokyselinovými zvyškami enzýmu izolovaných alkaloidov.